THE GLOBAL ENVIRONMENT MONITORING SYSTEM

GEMS
SAHEL SERIES
NUMBER 5

NAIROBI
1988

Inventory and Monitoring of Sahelian Pastoral Ecosystems

ANNEX 5:
MONITORING PASTURE PRODUCTION BY REMOTE SENSING

UNITED NATIONS ENVIRONMENT PROGRAMME
FOOD AND AGRICULTURAL ORGANISATION
GOVERNMENT OF SENEGAL

SAHEL SERIES

1. Introduction to Sahelian Pastoral Ecosystems Project
2. Rainfall in the Ferlo (Sahelian Region of North Senegal) since 1919
3. Use of Light Aircraft in the Inventory and Monitoring of Sahelian Pastoral Ecosystems
4. Sampling the Sahel
5. Monitoring Pasture Production by Remote Sensing
6. Inventory of Water Resources in the Ferlo
7. Woody Vegetation in the Sahel

THE GLOBAL ENVIRONMENT MONITORING SYSTEM

GEMS
SAHEL SERIES
NUMBER 5

NAIROBI
1988

Inventory and Monitoring of Sahelian Pastoral Ecosystems

ANNEX 5:
MONITORING PASTURE PRODUCTION BY REMOTE SENSING

UNITED NATIONS ENVIRONMENT PROGRAMME
FOOD AND AGRICULTURAL ORGANISATION
GOVERNMENT OF SENEGAL

Executive Summary:

The GEMS Sahel Series is a product of the Pilot Project for the Inventory and Monitoring of Sahelian Pastoral Ecosystems. This project was set up to demonstrate and assess the GEMS methodology for ecological monitoring in a West African pastoral ecosystem.

The present document, the fifth in the series, examines the use of radiometers in the estimation of primary production in sahelian pastures, based on the Project's results. It starts with a discussion of the principles and uses of the radiometer and a description of various types of radiometer. The data collected using a hand-held radiometer are treated in detail, and the efficiency of various indices examined in order to find one that is satisfactory for the estimation of green biomass in sahelian pastures. The report presents and discusses calibrated maps of green biomass production for five years, derived from satellite images of the Ferlo which were constructed from data collected by the Advanced Very High Resolution Radiometer carried on National Oceanographic and Atmospheric Administration satellites. The airborne instrument, for which no useable data emerged from the Project's activities, is given brief mention.

A glossary of terms connected to remote sensing and image processing and a list of acronyms and abbreviations commonly found in remote sensing literature are presented in annexe.

Global Environment Monitoring System Program Activity Centre
Sahel Series No 5

Title:

Monitoring pasture production by remote sensing

Author: M. Sharman

Target audiences: Development agencies
Range managers
Ecological monitoring projects
Remote sensing projects

Objectives:

(1) Presentation of method of radiometry for the measurement of biomass
(2) Presentation and discussion of results of hand-held radiometers in the Sahel, with particular emphasis on the utility of various radiometric indices in the estimation of biomass
(3) Discussion of the use of radiometers in light aircraft
(4) Presentation and discussion of results of satellite-borne radiometers in the Sahel

After working through whole strings of equations, in which the symbols stand for things whose intrinsic nature can never be known to us, he arives at last at a result which can be interpreted in terms of our own perceptions, and utilized to bring about desired effects in our daily lives.... The final conclusion is that we know very little, and yet it is astonishing that we know so much, and still more astonishing that so little knowledge can give us so much power.

Bertrand Russell. ABC of Relativity.

O dear Ophelia!
I am ill at these numbers:
I have not art to reckon my groans.

Shakespeare. Hamlet Act II Scene 2.

Frontispiece: The sahelian zone

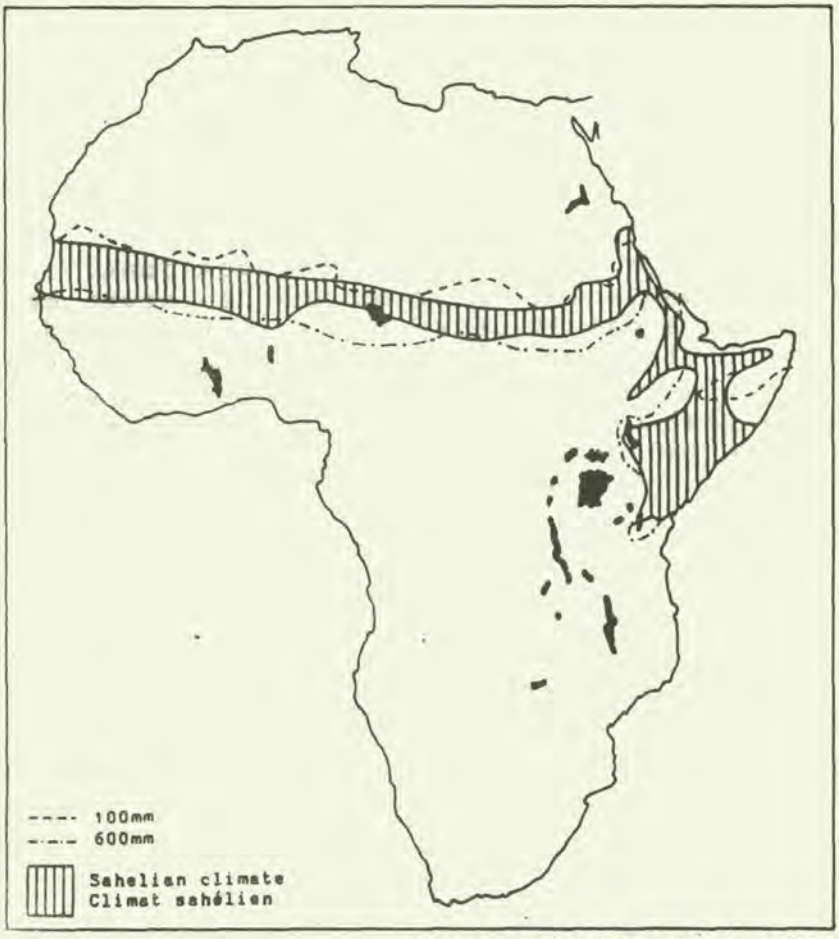

Source: Van Chi-Bonnardel R. (1973) L'Atlas de l'Afrique. IGN, Paris. Editions Jeune Afrique. Paris.

Preface

From the available data it seems probable that the numbers of domestic stock in the Sahel have reached levels equal to those of the decade before the catastrophic drought of 1968-72. At the same time the condition of the rangeland has improved only slightly, if at all, from its degraded state immediately after the drought. Furthermore, in parts of Africa, extension of agriculture has meant that pastoralists no longer have access to some of their former pastures. If the future of pastoral peoples is to be assured, the condition of rangelands must be preserved and if possible improved. Unfortunately the protection of the pastures poses well-nigh intractable social and complex ecological problems. The ecological problems alone cannot be solved unless the dynamics of the ecosystem are understood, and understanding can only be achieved by approaching the ecosystem as a functioning whole. To this end, the United Nations Environment Programme's Global Environment Monitoring System (GEMS) set up the Pilot Project for the Inventory and Monitoring of Sahelian Pastoral Ecosystems, which was executed by FAO as part of the global network of GEMS monitoring projects.

Objectives of the sahelian monitoring project

There were two major objectives. Firstly, the project was to adapt the standard GEMS ecological monitoring methods to the inventory and monitoring of sahelian pastoral ecosystems. Thus data were to be collected from observations made at three levels (on the ground, from the air, and from satellites), using methods designed to encourage a systems approach in their presentation and use. Secondly, the project was to collect data which would improve understanding of the renewable resources in the world's arid lands.

Choice of test zone

The ecology and economy of the north of Senegal is typically sahelian, and the area faces many of the ecological problems that confront the Sahel elsewhere. The zone chosen as a test area for the project, some 30,000 sq km of low-lying pastoral land (Figure 1), is bordered to the west by the shallow Lac de Guiers, to the north and east by the River Senegal, to the southwest by the fossil valley of the Ferlo, ending at Linguere, and to the south by the road between Linguere and Matam (on the River Senegal). This area corresponds roughly with that known traditionally as the Ferlo du nord, or north Ferlo. In the GEMS Sahel Series the test zone is known simply as the Ferlo.

Objectives of this document

This report aims to present the technique of remote sensing for the reader interested in a general account of its application to the measurement of primary production in pasturelands. It then sets out to examine and compare in some detail the various simple radiometric indices, using data collected in the field in Senegal. The use of airborne radiometers in initial experiments in Kenya is discussed. The use of a satellite-borne radiometer (the AVHRR of the NOAA series of satellites) in the measurement of primary production of the sahelian zone of Senegal is then examined.

Figure 1: Location of the test zone of the Pilot Project

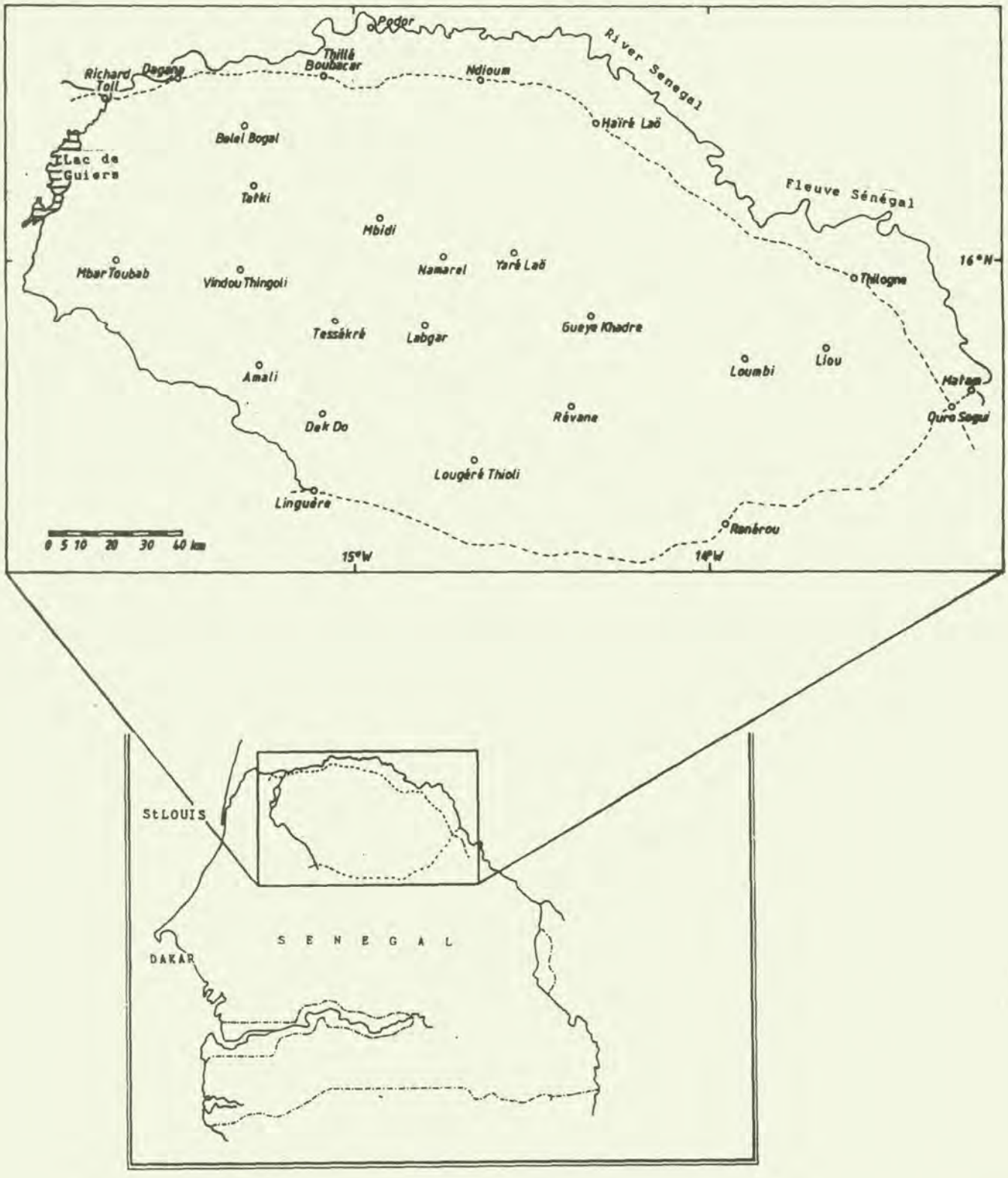

Monitoring pasture production by remote sensing

1 Introduction
1.1 The importance of standing biomass in the pastures of the Sahel
1.2 Measurement of biomass
1.3 Objective and balance of this report
1.4 Remote sensing and resource monitoring
2 Principles of the radiometer
3 Terminology
3.1 Remote sensing
3.2 Sensor, active and passive
3.3 Radiometer
3.4 Platforms
4 Atmospheric transparency and opacity: the atmospheric window
5 Statistical considerations
5.1 Transformations
5.2 Correlation
5.3 Repeated tests
6 The hand-held radiometer
6.1 Objectives of the study of the hand-held radiometer
6.2 Description of the instrument
6.3 Data collection
6.4 The hand-held radiometer in use
6.4.1 Calibration of the instrument
6.5 Data base
6.6 Frequency distributions and transformations
6.7 Visual estimates of biomass
6.8 Relationship between wet and dry weights
6.9 Radiometric measurements
6.9.1 Infrared
6.9.2 Red
6.9.3 Infrared minus Red
6.9.4 Ratio of Infrared to Red
6.9.5 Ratio of Infrared minus Red to Infrared plus Red (NDVI)
6.9.6 Ratio of IR - R to the square root of IR + R (NDIST)
6.9.7 The Perpendicular Vegetation Index (PVI)
6.9.8 Other indices
6.10 Improvements by considering species composition
6.10.1 Radiometric response of pure stands
6.10.2 Stands of graminaceous species
6.10.3 Stands of non-graminaceous species
6.10.4 Water content of stands
6.11 Naked earth
7 The air-borne instrument
8 The satellite borne instrument
8.1 Resolution requirements in ecological monitoring
8.2 Presentation of uncalibrated data
8.3 Sample distribution
8.4 Treatment of the data
8.5 Results
8.6 Calibration of the images
8.7 Presentation and use of calibrated data
8.8 The biomass maps of 1980-84
8.9 Use of the maps
9 Discussion

Table 1: Remote sensing uses of various bands of the electromagnetic spectrum
Table 2: Spectral bands detected by sensors on selected satellites
Table 3: Effect of transforming the data on the means and upper and lower 95% confidence limits
Table 4: R^2: Percent of variability explained by major axis of correlation of visual estimates with biomass
Table 5: R^2: Percent of variability explained by major axis of correlation of NDVI with biomass
Table 6: Mean dry biomass and 95% confidence limits estimated from four NDVI values. Confidence limits are taken from 95% confidence ellipse about data points
Table 7: Indices whose correlations with dry weight, wet weight and percent cover were greatest
Table 8: Slopes and elevations of major axis of correlation between production parameter and NDVI
Table 9: Slopes and elevations of major axis of correlation between production parameter and NDVI for all graminaceous stands
Table 10: Radiometric measurements on naked earth 12 July 1984
Table 11: Characteristics of various important earth-resources satellites and their on-board radiometers
Table 12: Estimates* of proportion of field area covered by each of 8 classes of NDVI values
Table 13: Annual correlations of NDVI class with dry weight and latitude
Table 14: Approximate values of biomass (kg/ha) represented by coloured areas on AVHRR NDVI images 1980-1983

==========

Figure 1: Location of field area: the Ferlo of north Senegal, West Africa
Figure 2: Frequency distributions of parameters measured in the Ferlo at the end of the growing seasons of 1981, 82 and 83.
Figure 3: Frequency distributions of wet and dry weight of clipped grass layer plants transformed by logarithm.
Figure 4: Correlation of Log Dry weight with Log Volume for all species.
Figure 5: Correlation of dry weight with wet weight for all species taken together
Figure 6: Frequency diagram of intensity of red and infrared light reflected from grass-layer plants at the end of the growing season in 1981, 82, and 83
Figure 7: Correlation of log(IR/R) and log(wet wt) for all species
Figure 8: Correlation of (IR-R)/(IR+R) with Dry weight for all species.
Figure 9: Correlation of (IR-R)/(IR+R) with Log Wet weight for all species.
Figure 10: Correlation of (IR-R)/(IR+R) with Log Dry weight for all species.
Figure 11: Correlation of $(IR-R)/\sqrt{(IR^2+R^2)}$ with Log Dry weight for all species.
Figure 12: Distribution of field samples of biomass collected in 1980-1983 for the calibration of AVHRR images
Figure 13: Frequency distribution of dry weight of samples collected for calibration of AVHRR images
Figure 14a: Correlation of NDVI class with dry weight (kg/ha)

for 1980-1983: eight classes
Figure 14b: Correlation of NDVI class with dry weight (kg/ha): medians and interquartile ranges for eight classes 1980-1983
Figure 15: Correlation of NDVI class with dry weight (kg/ha): medians and interquartile ranges for six classes 1980-1983
Figure 16a: Correlation of NDVI class with logarithm of dry weight for 1980-1983: six classes
Figure 16b: Correlation of NDVI class with dry weight (kg/ha): medians and interquartile ranges for six classes 1980-1983
Figure 17a and 17b: Biomass of the grass layer of the Ferlo at the end of the rainy seasons of 1980 and 1981
Figure 18a and 18b: Biomass of the grass layer of the Ferlo at the end of the rainy seasons of 1982 and 1983
Figure 19a and 19b: Biomass of the grass layer of the Ferlo at the end of the rainy season 1984 and key to Figures 17-19

==========

Appendix 1: Glossary of terms connected to remote sensing and image processing.

1 Introduction

1.1 The importance of standing biomass in the pastures of the Sahel

Increasingly, in response to the steady deterioration of the rangelands, the Governments of the sahelian countries are establishing Projects for the management of livestock in these semi-arid pastures. In the Sahel the fodder available at the end of the growing season in a given area can change from over 2000kg/ha in one year to less than 50kg/ha the next. The biomass of standing grass-layer plants therefore often largely (but not entirely) determines the usefulness of the pastures.

Knowledge of the quantity and distribution of fodder is thus a prerequisite for the efficient management of a pastoral ecosystem, since it not only helps to determine stocking rates and stock movement, but is also as an indicator of the condition of the rangeland (GEMS 1986d). While the pastoralist will discover rapidly by word of mouth where the good pastures are to be found each year, and if necessary arrange to move his herd accordingly, planners and developpers need quantified data including those that can be supplied by an ecological monitoring unit using the various techniques available for the measurement of biomass.

1.2 Measurement of biomass

Biomass may be measured by several methods, the most accurate and laborious being to clip and weigh samples of the sward. A far less onerous method is provided by remote sensing (Kumar and Monteith 1982, Tucker 1980).

1.3 Objective and balance of this report

The objective of this report is to examine the use of radiometers in the estimation of primary production in sahelian pastures, based on the results of the Project in north Senegal.

Ideally, the attention given to the use of instruments on the ground, in the air and in orbit would be in proportion to their utility as judged from the results of the Project. However, in practice the data available to the Project has led to a regrettably lopsided report; the use of the hand-held radiometer is treated in most detail, that of the satellite instrument in less detail, and the airborne instrument, for which no useable data emerged from the Project's activities, is given only brief mention.

The problems involved in obtaining a representative sample of the standing grass biomass in a vast area of natural pasturelands are not discussed here, since they are examined in detail in GEMS (1986d).

1.4 Remote sensing and resource monitoring

Although in this report we are exclusively concerned with the use of the radiometer for estimating the production of fodder in sahelian pastures, remote sensing has proved useful in the inventory or monitoring of other parameters, especially in the field of meteorology (perhaps its most familiar application to those who watch the weather forecast on TV), oceanography, hydrology and geology, cartography and land use, agriculture and the monitoring of crops and natural vegetation.

2 Principles of the radiometer

All radiometers depend on the photoelectric effect: photons falling on a suitable receptor liberate electrons. If the radiation is absorbed near a potential barrier, such as a p-n junction, a potential difference is established across the barrier and can be measured and recorded.

Most radiometers measure incident energy in several separate bands of the spectrum, which has the advantage that the intensity of the energy reflected or emitted from a surface in two or more bands can then be compared. This will normally give more information about the surface than would a single measure summing the energy in the several bands.

The use of the radiometer in the measurement of green biomass depends on the influence of photosynthesising plants on the radiation reflected from them. Actively photosynthesising chlorophyll molecules absorb light in several discrete bands of the spectrum, the most important of which (due to chlorophyll α) is at about 675nm (Rabinowitch 1958). The cell walls of plants reflect strongly in the near infra-red (between 750 and 1100nm), a feature that familiar to everone who has seen false-colour infrared images of vegetation. An instrument capable of detecting and measuring the intensity of energy in these two wavebands (R at 675nm and IR at 800nm) is therefore capable of measuring an index proportional to the surface area of plant matter (reflectance in the infrared) and one inversely proportional to the activity of the chlorophyll in that plant matter (reflectance in the red). This is the principle of the radiometer or remote sensing method of estimating biomass.

3 Terminology

The specialised vocabularies of remote sensing, and the field of image processing so necessary to satellite and airborne remote sensing, are large enough to warrant a glossary (Appendix 1). However, it is convenient to define here:

3.1 Remote sensing

Remote sensing is the detection and recording of electromagnetic information by means of an artificial sensor which is not in contact with the object from which the information is collected.

3.2 Sensor, active and passive

A sensor is a device which detects and records levels or changes in some quantity.

The electromagnetic sensor may be any one of several devices, whose most familiar manefestations include the photographic light-meter, the camera and the video recorder. These are passive sensors, ones which detect and record energy radiated or reflected from surfaces without the need for the device itself to emit radiation. Radar is a well-known example of an active remote sensor, that is, one which emits its own electromagnetic radiation and monitors the reflection.

3.3 Radiometer

The term "radiometer" could be applied to any manmade, passive remote sensing device which measures the intensity of incident electromagnetic energy, but in practice it is not normally used to describe photographic light meters.

3.4 Platforms

Originally, the word "platform" described the bed on which the radiometer was mounted, but the term has come to be used for the vehicle in which it is carried or even the height above the ground at which it is used. For most ecological applications the sensor is carried on one of four platforms: by hand or mounted on a tripod; in an aircraft; or in a satellite.

While the products of airborne sensors (especially the familiar false-colour infra-red images of vegetation) are known to a wide public, satellite images have proved so useful and have caught the popular imagination to such an extent that a major product of satellite remote sensing is known to perhaps a quarter of the world's population. By contrast, the hand-held radiometer is known to the general public only in the form of photometers.

4 Atmospheric transparency and opacity: the atmospheric window

The atmosphere is not uniformly transparent to all wavelengths in the electromagnetic spectrum. It is particularly transparent in the near ultraviolet, the visible, and near infrared, and exhibits transparent windows in the short-wavelength and mid infrared. It is generally opaque in the far infrared and becomes transparent once more in the microwave frequencies.

Remote sensing, especially from orbit and high-altitude aircraft, is therefore restricted to certain bands of the electromagnetic spectrum - in those windows of atmospheric transparency (Table 1). Hand-held radiometers, and those carried in low-flying aircraft, are now

Table 1: Remote Sensing uses of various bands of the electromagnetic spectrum

Wavelength (μm)		
0.4	Atmosphere scatters light of these wavelengths Chlorophyll absorbs strongly	Violet
0.5		Visible light
0.6	Plant cell walls reflect strongly	
0.7	Chlorophyll absorbs strongly	Red
0.8	Plant cell walls reflect very strongly. Distinction can be made between Broadleaf/needleleaf plants	Near Infrared
0.9		
1.0	Distinction can be made between clear and turbid water	
1.1	Distinction can be made between fresh snow and dirty snow or ice	
1.2		
1.3	Dry soil reflects more strongly than does wet soil	Short-wavelength Infrared
1.4		
	Atmosphere opaque	

frequently designed to detect energy in the same bands as do the satellite sensors (Table 2), so that the measurements can be compared.

5 Statistical considerations

5.1 Transformations

In the analyses undertaken in the course of the preparation of this report many cases were found in which the frequency distributions of the parameters measured were not Gaussian (or Normal - see glossary). In order to use parametric statistics, it is necessary to transform the parameter in such a way that the resulting transformed data meet the assumptions of the analyses.

To many non-statisticians, transformations seem suspiciously like data "massage", that is, the squeezing of a statistically significant result out of recalcitrant data by some arcane and unjustified manipulation of the original numbers. However, in a sense transformations do not alter the data at all; all that is altered is the scale on which they are expressed. The (familiar but entirely arbitrary) linear scale is replaced by a square root, inverse, logarithmic, arcsine or other scale chosen so that the data become more Normally distributed over the scale than they were over the linear scale.

For example, it may be that many of the original numbers in the data are crowded together near the low end of the range of the data, and very few are scattered over the upper reaches. In this case, by using a logarithmic scale it may be possible to bring out the otherwise hidden observation that within the crowded low values, there are in fact very few with extremely low values, and that most measurements are grouped around the middle of the range on this transformed scale.

Thus, the first step before starting to examine correlations between variables is to plot the frequency distributions of the data and to examine them to see whether they are Gaussian or whether some simple transform can be used to Normalize them.

Transformations are discussed in greater detail in many texts on parametric statistics (eg Pollard 1977, Sokal and Rohlf 1969).

5.2 Correlation

The intention of the analyses in this document is to establish the degree of association between biomass and various estimators. Since biomass is clearly independent of the estimator, it might seem appropriate to use regression techniques in the analysis. However, since the biomass is not measured without error (in the statistical sense), an underlying assumption and prerequisite of regression, it is correct to use correlation and not regression (Sokal and Rohlf 1969:495). In those cases for which it was of interest, the technique of principal or major axis (Sokal and Rohlf 1969:526) was used to characterise the trend of the scattered points by the line which passed through the centroid of the cloud and through its longest dimension.

5.3 Repeated tests

In the section examining the efficiency of various radiometric indices it is inevitable that the same data are used repeatedly for different tests; if it were not so, direct comparison between the estimators would not be straightforward. However, this means that the significance levels of the results of the repeated tests are greater than they would be for a single test, and should not be relied upon (Pollard 1977:135).

6 The hand-held radiometer

Handheld radiometers, and some of the radiometers used from aircraft, are normally used to detect (and perhaps record) the pooled intensity of radiation reflected in the sensed wavebands from all the surfaces in the scene (Daughtry et al 1983). Each scene is therefore represented by a single value in each sensed waveband, and the instrument is not designed to construct an image of the scene.

The details of radiometer construction and the wavelengths to which they are sensitive depend on the purpose for which they are built. Of particular interest to ecological monitoring units are those which are sensitive to those bands in the red and infrared which are absorbed by chlorophyll and reflected by cell walls, respectively.

6.1 Objectives of the study of the hand-held radiometer

This report presents the results of a study in the sahelian north of Senegal (Figure 1), carried out by the Pilot Project for the Inventory and Monitoring of Sahelian Pastoral Ecosystems (GEMS 1986a, Le Houérou 1986), to test the use of a hand-held radiometer constructed and loaned to the Project by NASA, and the use of AVHRR images from NOAA (previously TIROS-N) satellites.

Clearly the use of a radiometer or any other method involving costly equipment or time-consuming methods is only justifiable if it gives results which are more accurate and precise than those which can be gathered by rapid visual estimates. Field data, including visual estimates of cover and height, were collected in the three years 1981-1983 with the aim of comparing these estimates against those made using the radiometer.

Secondly, various indices derived from the measures of reflected radiation in wavebands near 675μm (red light or R) and 800μm (infrared or IR) have been proposed and tested, usually considering the radiometric responses of a single-species sward of plants at the same phenological stage. The simplest of these indices is the intensity of red light (or its inverse) reflected by the plant, and next-simplest is the ratio IR/R (Pearson et al. 1976). This second ratio has largely been superceded by the index (IR-R)/(IR+R), called the Normalised Difference Vegetation Index (NDVI) by Tucker (1980). These and other

indices are worth investigating in sahelian pastures, in which mixed-species swards of grass-layer plants, at various phenological stages, are the rule rather than the exception.

6.2 Description of the instrument

The instrument used by the Project was constructed with band-pass filters making it sensitive to bands corresponding to channels 1, 2 and 3 of the AVHRR on NOAA satellites, that is, to light of wavelengths of about 0.55-0.68 µm, 0.73-1.10 µm and 3.55-3.93 µm respectively.

Like other hand-held radiometers (see Holmes 1970 or Lee 1975 for reviews) the one used by the Project consisted of a probe with a pistol grip, connected to a box containing the power source, electronics and liquid-crystal digital readouts for the three channels. This box can be slung from the shoulder on a bandolier. The light weight of the instrument and its independence of external power sources makes it ideal for use in the field at a distance from roads or motorable tracks.

The sensor is fitted with moveable diaphragms which will optionally restrict the field of view to within 6° or 12° of the optical axis, which, at 130cm (roughly shoulder height) from the ground, means that its target covers an area of about 600 sq cm or 2.4 sq m respectively. For the probe to sense an area of 1 sq m at this height the diagaphragm would need to restrict the field of view to within 7.8° of the optical axis; alternatively, with a 6° field of view, the instrument should be held about 170cm above the ground. This corresponds roughly to eye level for a person of 180-185cm.

6.3 Data collection

For the measurement of the biomass of the grass layer and the calibration of NOAA AVHRR satellite images the Project used a simple sampling design designed to gather samples from as wide an area of its test zone in as short a time as possible.

The test zone is crisscrossed by firebreaks used mainly for communication. At intervals of ten kilometers along selected firebreaks the Project chose a site, about 100m from the firebreak, at which the biomass of the grass layer seemed representative of that seen in the previous one or two kilometers.

At each station 5 to 13 plots of one square metre were located by selecting areas which seemed representative of the station. In each plot the mean values of various parameters characteristic of the grass layer were estimated or measured. These parameters included the identity of the two species with the greatest cover, visual estimates of the percent cover (defined as the percent of the ground covered by a vertical projection of all green matter in the plot) and the mean height of the stand, its clipped wet weight, and the reflectivity of the sward in the red and infrared bands of the spectrum. The clipped samples were taken back to the laboratory and dried in an oven at 95°C for 24 hours, after which they were again weighed.

6.4 The hand-held radiometer in use

Since the instrument is intended to record radiation reflected off the leaves of plants, the sun should be high in the sky (since leaves are non-Lambertian reflectors and sun angle will affect the readings) and there should ideally be no haze and certainly no overcast. The readings from the instrument are calibrated for ideally reflected radiation (section 6.4.1) before each use. The operator then stands facing the sun and extends the probe at shoulder height, so that is poised over the vegetaion sample, pointing as near vertically at the ground as possible. The readings on the displays are recorded by a second person. After the data on the radiometric response of the vegetation are collected, a second set of calibration readings are taken to measure ideally reflected radiation.

6.4.1 Calibration of the instrument

The ideally reflected radiation at the time of each reading is recorded by taking calibration readings from a surface which is as nearly as possible a Lambertian reflector. For the purposes of the Project, this was a sheet of steel coated with barium sulphide paint. This surface is fragile and easily made dirty, and it is important to protect the plate from dust and scuffs.

Readings from the ideal reflector are taken both immediately before and after each measurement of radiation reflected from the vegetation, and the ideally reflected light at the time of the measurement is taken to be the mean of the two calibration readings. Correction for varying intensities of incident light can therefore be made by dividing the value recorded for a given channel by the mean calibration reading for that channel.

6.5 Data base

Three field trips were undertaken, in 1981, 82 and 83. Data were collected at a total of 544 plots (183, 238 and 123 respectively). Results from individual years are presented in Sharman and Vanpraet (1983). In this document, results for all three years are pooled.

6.6 Frequency distributions and transformations

Primary production in the Sahel is characterised by wide areas in which cover and biomass is predominantly relatively poor, interspersed by scattered patches of higher production. This heterogeneous production is brought out graphically by the frequency distributions of the data recorded in the field (Figure 2), in which low values for all the measures were more frequent than were mid-range or high values.

Table 2: Spectral bands detected by sensors on selected satellites

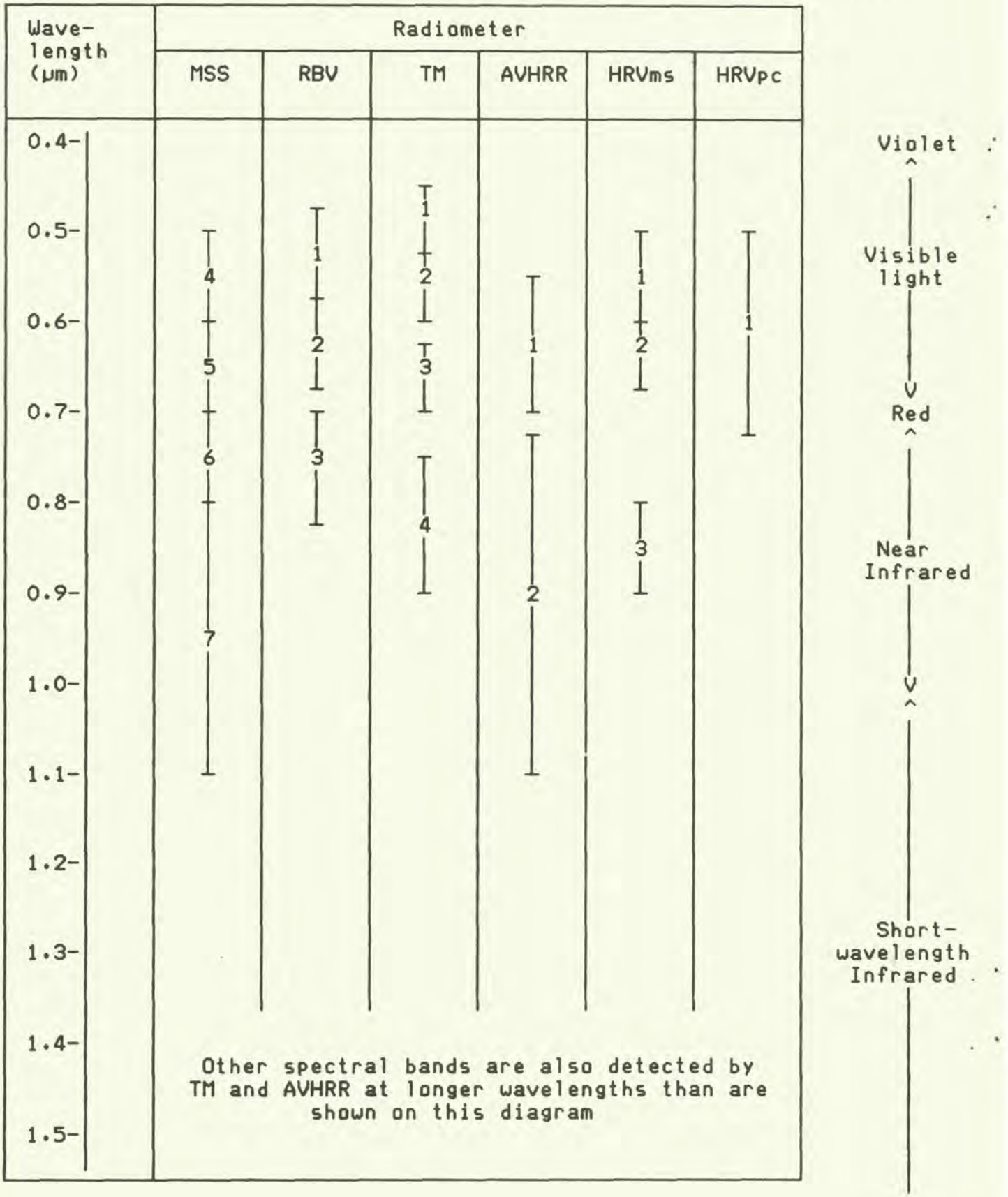

Figure 2: Frequency distributions of parameters measured in the Ferlo at the end of the growing seasons of 1981, 82 and 83.

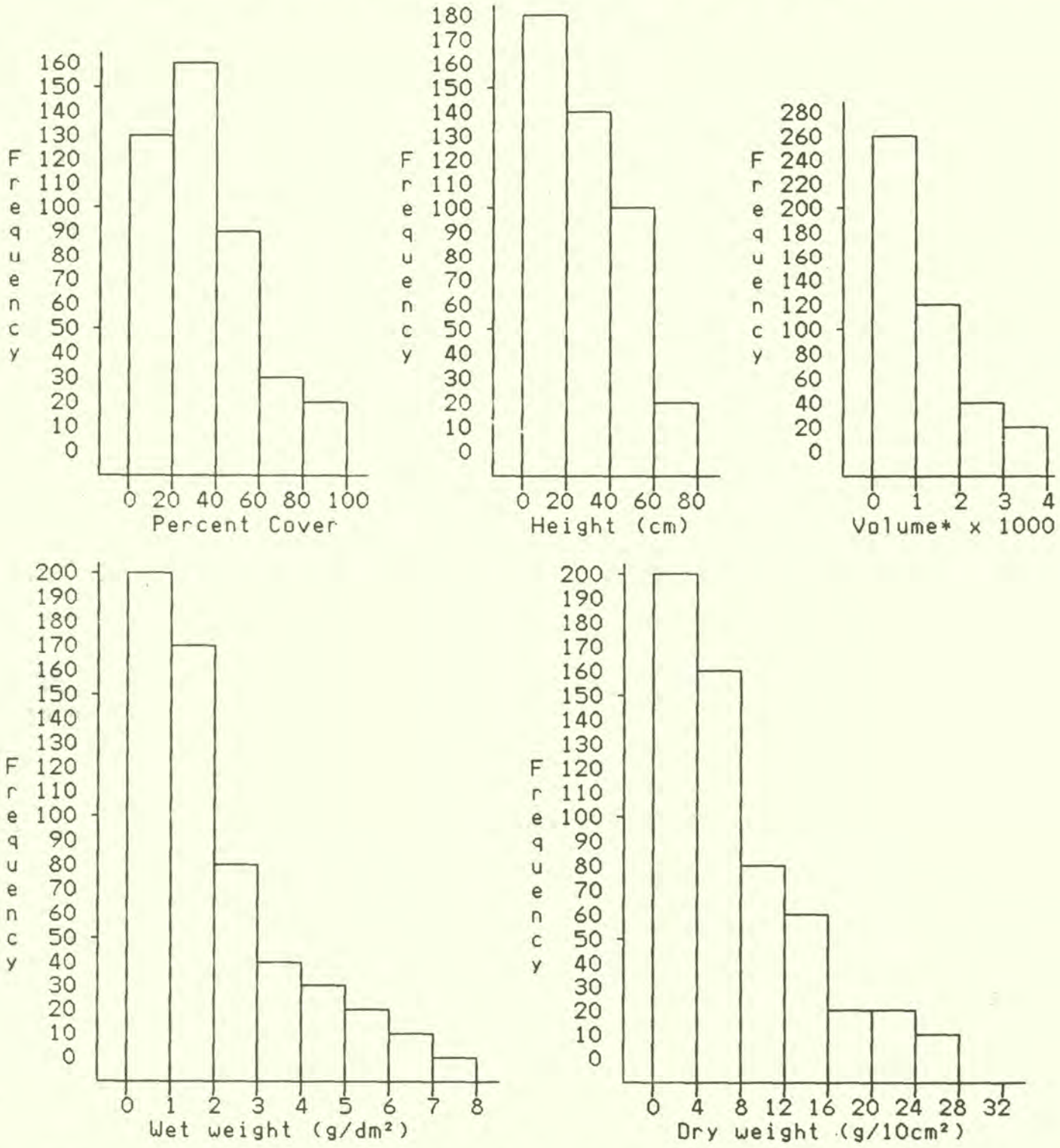

* Volume was calculated by multiplying % cover by height of the sward

The frequency distributions of five of the six non-radiometric parameters were so skew that the lower 95% confidence limit of the untransformed data was negative (Table 3). This was avoided by transforming the data by logarithmic or arcsine transforms, the transform being chosen in part by consideration of the shape of the untransformed distribution. Figure 3 presents graphically the Normalizing effect of transforming the scale on which weights are expressed from linear to logarithmic. The resulting 95% confidence limits are not symmetrical about the mean, and the upper confidence limits of logarithmically transformed data are likely to exceed those of the untransformed data (Table 3).

The same transforms were used in the study of correlations in the data.

6.7 Visual estimates of biomass

The results of the field work in the Ferlo show that neither the proportion of the ground covered by the vertical projection of the aerial parts of the vegetation nor the height of the sward are by themselves particularly good estimators of biomass. The best visual estimate of the biomass available from these data is given by calculating a measure of volume (percent cover multiplied by mean height of the sward). This measure accounts for almost 60% of the variability in the wet biomass (Table 4) and when transformed by logarithms accounts for over 70% of the variability of the logarithm of the dry biomass.

Nevertheless, while the relationship between log(biomass) and log(volume) is satisfactorily linear (Figure 4), the spread of values of biomass estimated by this parameter remains large. For the data collected in the Ferlo, a median value of log(volume) is around 6, corresponding to values of log(biomass) ranging from about 2.6 to 4.9, or from 13.1 g/m² to 129 g/m². It is unlikely that this tenfold spread of values is satisfactory for many ecological monitoring purposes, unless very many estimations are made, allowing, in this case, the "average" value of about 41 g/m² to be used.

For the data collected in the Ferlo, the logarithm of the biomass can be calculated from the logarithm of the volume with the equation:

$$\log(\text{biomass}) = 0.651 * \log(\text{vol}) - 0.203$$

where * stands for multiplication; or the biomass can be calculated from the volume by:

$$\text{biomass} = \text{vol}^{0.651} * e^{-0.203}$$

where e, the base of natural logarithms, is roughly 2.718, so that:

$$\text{biomass} = 0.816 * \text{vol}^{0.651}$$

Table 3: Effect of transforming the data on the means and upper and lower 95% confidence limits

Parameter	Unit	No transform			With transform			
		lower 95% cl	mean	upper 95% cl	name	lower 95% cl	mean	upper 95% cl
Cover	%	-8.6	31.3	71.3	Arcsin	1.5	30.1	74.4
Height	cm	-8.4	27.4	53.2	Log	5.5	22.2	89.2
Volume	*	-1137	1040	3215	Log	80.1	564	6176
Water cont	%	25.9	55.7	85.6	Arcsin	23.6	55.5	85.1
Wet weight	g/m	-170.5	192.3	555.0	Log	21.5	129.7	781.1
Dry weight	g/m	-57.2	77.1	211.5	Log	10.0	54.4	295.1
* volume was calculated b multiplying % cover by height of the sward								

The arcsine or angular transformation is used, with data measuring percentages or proportions, to prevent the variance being a function of the mean. It is calculated by finding the angle whose sine is equal to the square root of the datum expressed as a proportion. In the computer treatment of data using a language which provides the inverse tangent but not the inverse sine, the transform is calculated from:

Arcsine(SQUARE ROOT(P))=Arctan(SQUARE ROOT(P/(1-P)))

==========

Table 4: R^2: Percent of variability explained by major axis of correlation of visual estimates with biomass

	Wet wt	Log Wet wt	Dry wt	Log Dry wt
% Cover	44	47	46	46
Height	48	52	54	59
Volume	59	51	66	55
Arcsine % Cover	44	48	45	47
Log Height	36	49	41	58
Log Volume	49	66	53	72

sample size=438

Figure 3: Frequency distributions of wet and dry weight of clipped grass layer plants transformed by logarithm.

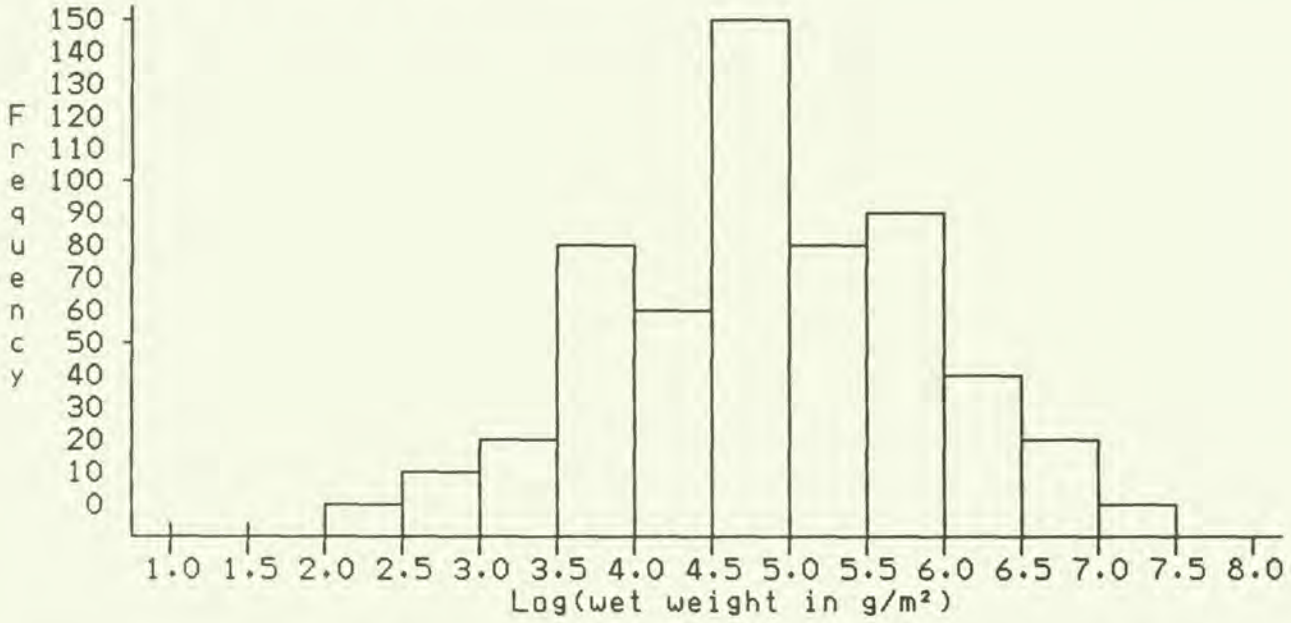

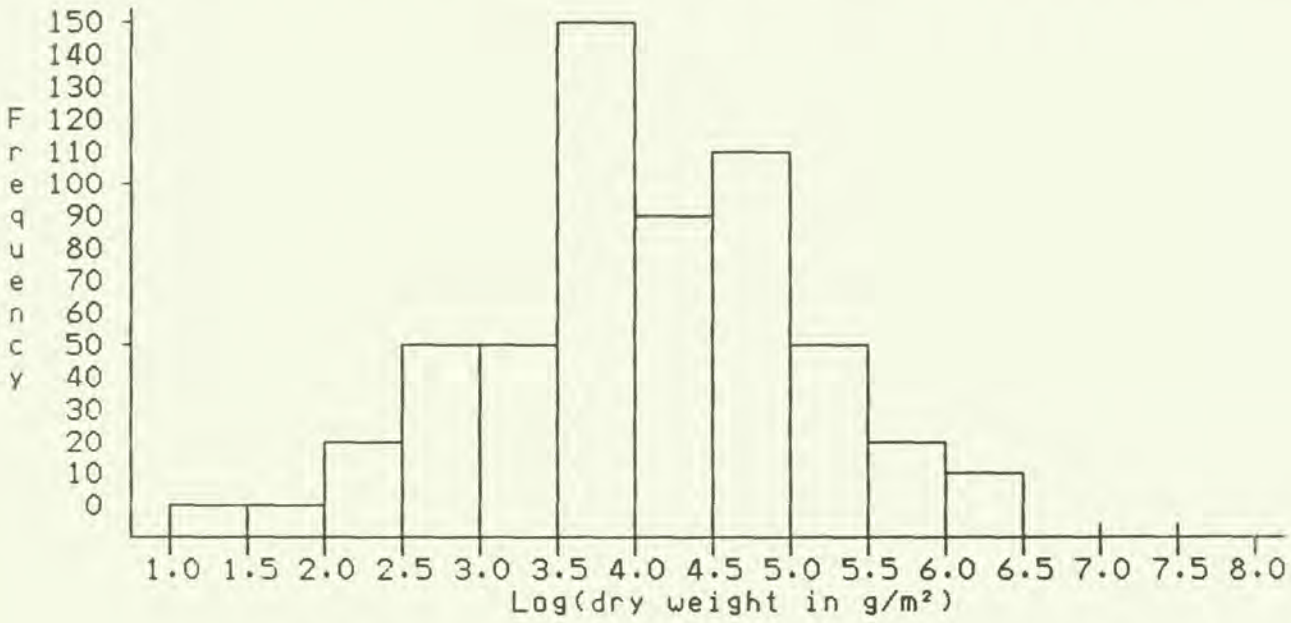

Figure 4: Correlation of Log Dry weight with Log Volume for all species.

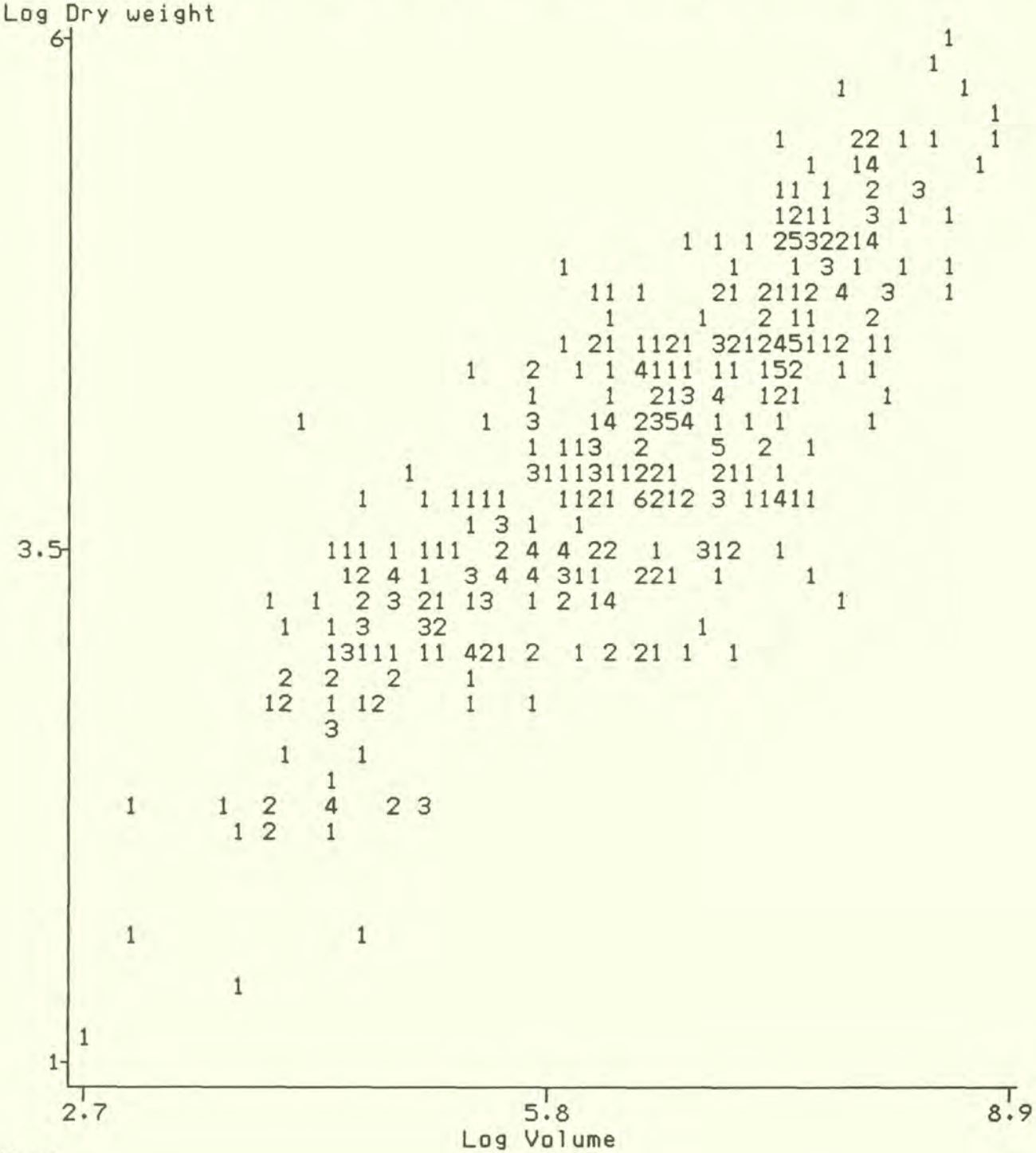

Key:

1=single data point in this row and column of the printer
2=two data share this location
3=three (etc)

Product-moment correlation coefficient
r = 0.846 d.f. = 436 t = 25.930 (p < 0.001)
Equation of major axis: y= .651 * x -.203

6.8 Relationship between wet and dry weights

In the samples collected in the Ferlo, the dry weight could be estimated from the wet weight by multiplying the wet weight (expressed in g/m^2) by 0.35 and adding 9.7. The correlation between the two measures explained about 87% of the variance in the dry weights. However, it will be seen in the following analyses that despite the high correlation between wet and dry weights (Figure 5), all the radiometric estimators of biomass are more highly correlated with wet weights than they are with dry weights.

The relationship between dry and wet weights is clearly of no general use, since the water content of the plants depends not only on their species composition but also on their phenological state, which in turn depends on the time of year at which they are collected.

6.9 Radiometric measurements

Although data were collected on three channels, only two (red and infrared) are examined here.

Since red light is absorbed by chlorophyll, and infrared is reflected by the cell walls, the simplest radiometric index that is likely to be correlated with biomass is either 1/R or IR. Given that the intensity of infrared light is proportional to the leaf area as seen from the sensor, and that of red light is inversely proportional to the degree of chlorophyll activity, an obvious second candidate for a radiometric index probably correlated with biomass is simply IR/R.

Figure 6 shows that the energy of the reflected infrared light tended to be higher than that of red light, and further examination of the data shows that in 98% of the readings the intensity of infrared light fell above the line defined by

$$\text{Infrared} = 0.91 * \text{Red} + 0.11$$

Since the intensity of red light did not exceed 0.67, any index based on the difference of the two bands will be positive if R is subtracted from IR, and greater than 1 if IR is divided by R.

A third candidate index is suggested by considering the difference in energy in the two bands IR-R. However, this index will tend to the value of IR, since R is typically smaller than IR, and may therefore contain little more information than IR alone.

By dividing IR-R by the sum of the energy in the two bands, IR+R, an index results (Rouse et al 1973) with the property that no matter what the values of IR and R, its value is limited by +1 and -1. In practice, with typical IR and R measurements from vegetation, the index varies between 0 and 1; as the value of R approaches that of IR, the index tends to zero. As R becomes very small relative to IR, the index, called the "normalized difference vegetation index", or NDVI, by Tucker (1979), tends to 1. The index therefore increases as more red light is

Figure 5: Correlation of dry weight with wet weight for all species taken together

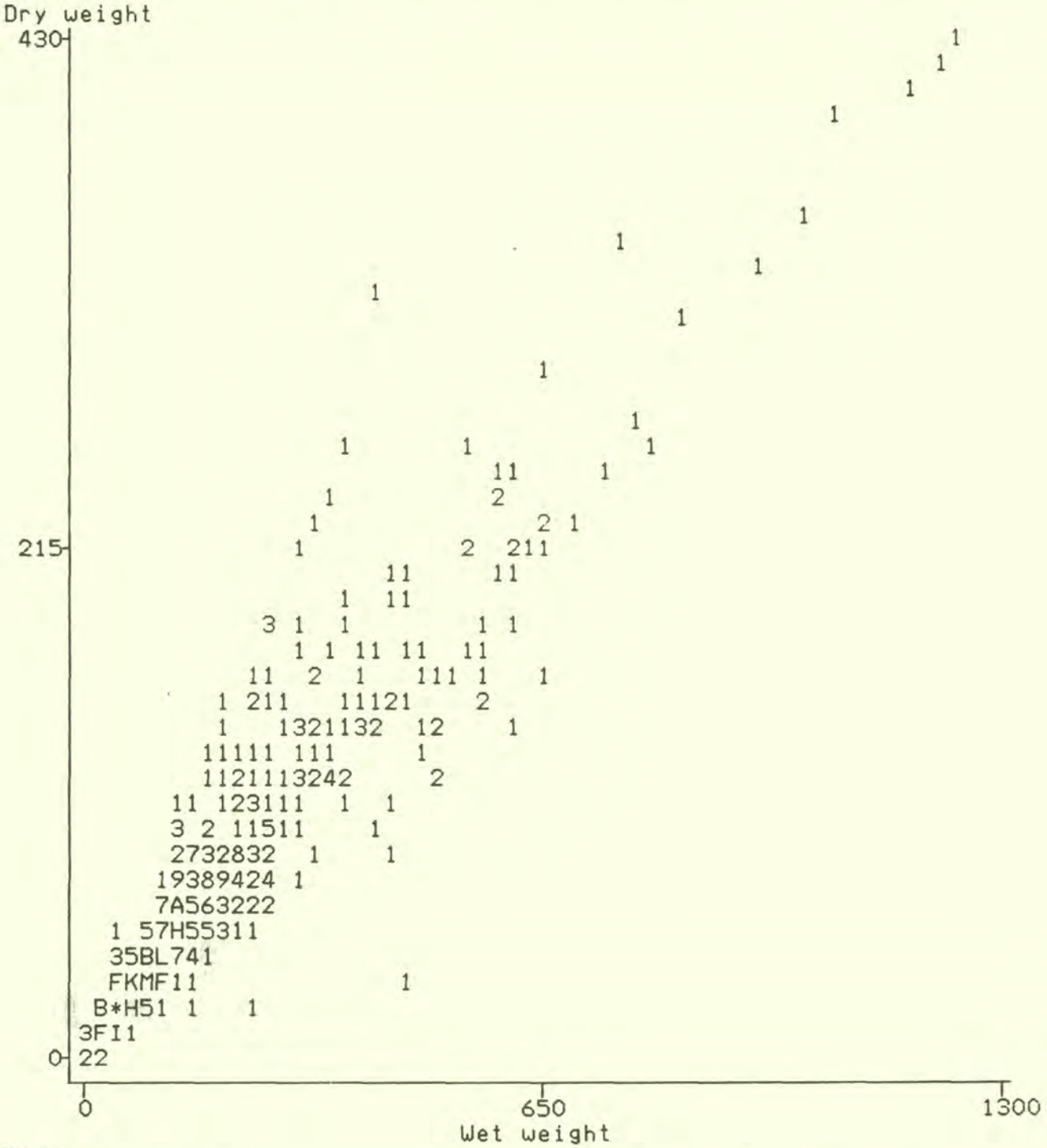

Key:

1=single data point in this row and column of the printer
2=two data share this location
3=three (etc)
A=ten data share this location
B=eleven (etc)
*=28 data share this location

Product-moment correlation coefficient
r = 0.932 d.f. = 542 t = 38.865 (p < 0.001)
Equation of major axis: y= .351 * x + 9.699

Figure 6: Frequency diagram of intensity of red and infrared light reflected from grass-layer plants at the end of the growing season in 1981, 82, and 83

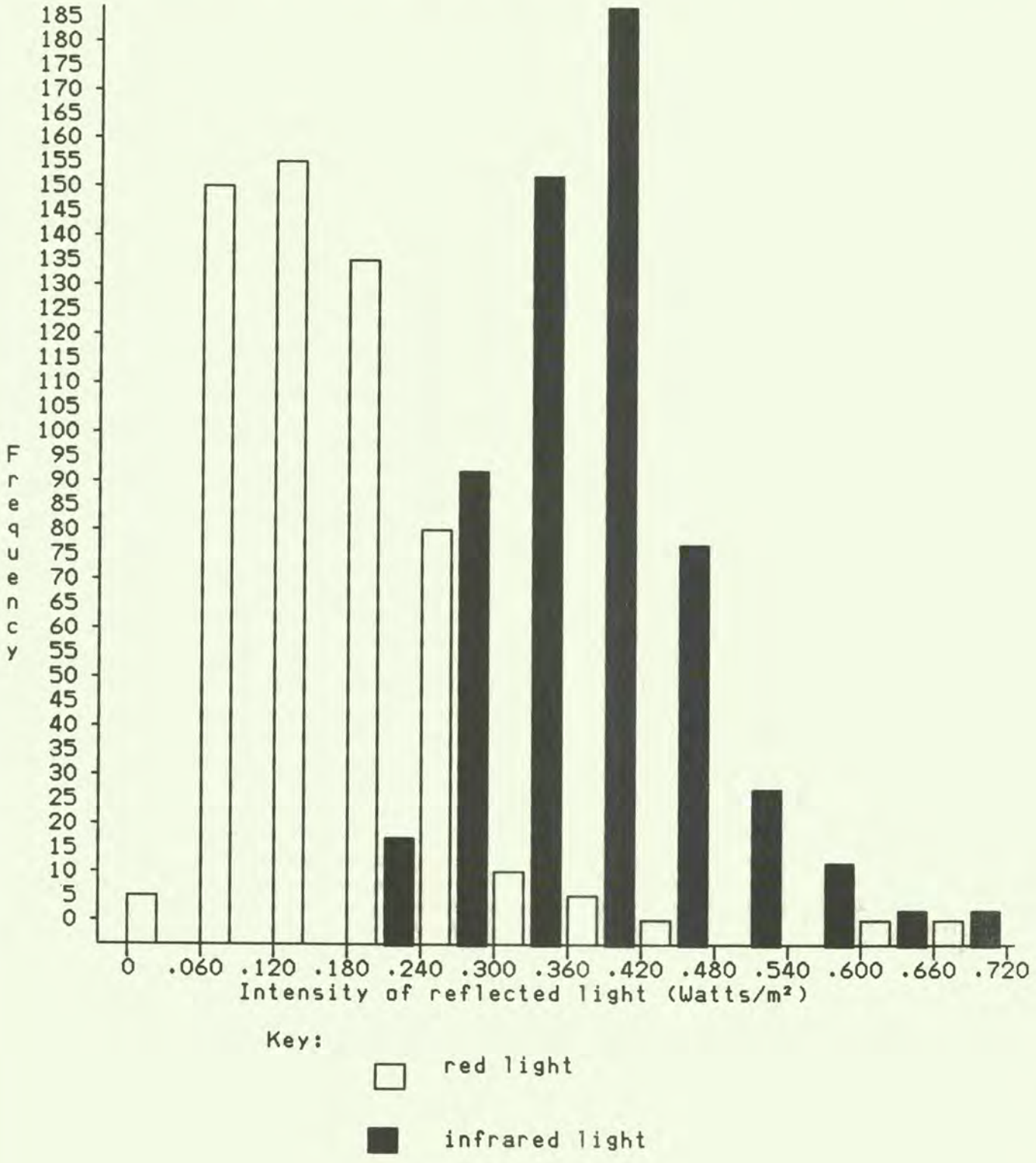

absorbed by the vegetation, that is, the more active chlorophyll is present in the target area.

Algebraically, (IR-R)/(IR+R) can be rewritten as

$$(IR/R-1)/(IR/R+1)$$

and it may be seen that the NDVI contains no information not contained in the more direct ratio. Nevertheless, the index will not be correlated with biomass in the same way as is IR/R since, relative to IR/R, the NDVI will tend to "stretch out" at low values of biomass, as can be seen by plotting the graph of $y=(x-1)/(x+1)$.

The frequency distribution of the NDVI can be Normalized in the statistical sense by a square root transform.

The difference between the energy in the two bands, IR-R, can also be "normalized" by the distance between them $\sqrt{(IR^2+R^2)}$. The resulting "difference normalized by distance" index (NDIST) is clearly closely related to the NDVI, but when IR/R is small (between 1 and 3) increments in the value of the ratio IR/R cause the NDIST to change more rapidly than does the NDVI. This may make it particularly suitable to low-biomass swards, for which values of IR/R are frequently below 3. The ratio between the NDIST and the NDVI alters from near 1.414 to 1 over the range of values IR/R typical of the data.

All of these indices - and several others derived from the IR and R readings collected in the field - were correlated against both wet and dry weight of their corresponding samples. Since the radiometer may be responding more directly to the percentage cover than to the biomass, this relationship was also examined. Dry plants may reflect infrared but are unlikely to absorb red light since they will not be photosynthesising, and the relationships were therefore reexamined, excluding all plants for which the water content was less than 30%.

6.9.1 Infrared

The intensity of infrared light reflected from the vegetation was poorly correlated or uncorrelated with any measures of biomass, cover, height of the sward or volume. R^2, the proportion of the variability in the infrared reflection explained by vegetation measures, never exceeded 8%; normally at least 50% must be explained by the correlation for the one variable to be considered a useful estimator of the other. Although the form of the scatergrams suggested that the inverse of the intensity of infrared light might be correlated in some cases, this proved not to be the case (R^2 always $< 10\%$); the intensity of reflected infrared light is surprisingly unrelated to any measures of the vegetation production collected by the project.

6.9.2 Red

The intensity of red light was inversely correlated with all the vegetation measures, particularly those of percent cover ($R^2=39\%$) and wet weight ($R^2=48\%$). Its utility as a measure of dry weight was more limited ($R^2=38\%$).

6.9.3 Infrared minus Red

In no case was IR-R as good an estimator of any vegetation parameter as 1/R on its own.

6.9.4 Ratio of Infrared to Red

The ratio IR/R was a reasonably good estimator of wet weight (R^2=54%) and its logarithm a better estimator of the logarithm of wet weight (R^2=64%). The correlation between log(IR/R) and log(wet wt) is given in Figure 7. A clear trend for higher cover to give higher IR/R values was detected (R^2=42%). Unfortunately this trend is of little ecological use because while very low cover, of the order of 0 to 20%, gave consistently low values of IR/R (typically between 1.6 and 2.6), increased cover gave erratic IR/R values. At 50% cover, readings as low as 2 were frequently observed, but readings up to 6.9 were also recorded. Only five plots were scored as having complete cover, but the values of IR/R for these plots ranged from 3.1 to 8.8, which was also the highest value of IR/R recorded in these data.

6.9.5 Ratio of Infrared minus Red to Infrared plus Red (NDVI)

The ratio (IR-R)/(IR+R), or NDVI, was better correlated with wet weight than it was with dry weight (R^2=60% and 48% respectively). It was also quite closely correlated with percent cover (R^2=50%). The form of the correlations (that of NDVI and dry weight is shown in Figure 8) suggested that the ratio was becoming less responsive to higher values of biomass; that is, that an increment in the weight (and hence height) of the grass layer plants was less effectivly monitored in swards with a relatively large biomass than it was in swards with poor production.

The effect of this in practical terms is that while low values of the NDVI give relatively precise estimates of dry weight, high NDVI values are extremely imprecise (Figure 8). Thus, for example, an NDVI of .22 may be recorded from a biomass of between about 3g/m² (that is, effectively naked earth) and 65g/m², while vegetation whose dry weight is anywhere between 22.5g/m² and 290g/m² may give rise to an NDVI of .5. Since, in the Ferlo at least, pasture whose dry weight is less than 200g/m² is likely to be grazed out long before the end of the dry season, the levels of production over which the measure is precise are of little interest for ecological monitoring.

This typically curvilinear relationship suggests that the index might be better correlated with the logarithm of the wet weight (Figure 9), and indeed the NDVI is particularly well correlated with log(wet wt) (Table 5), for which 67% of the variance in the data is explained. The NDVI is therefore marginally better than the index IR/R for the estimation of wet weight.

Figure 7: Correlation of log(IR/R) and log(wet wt) for all species

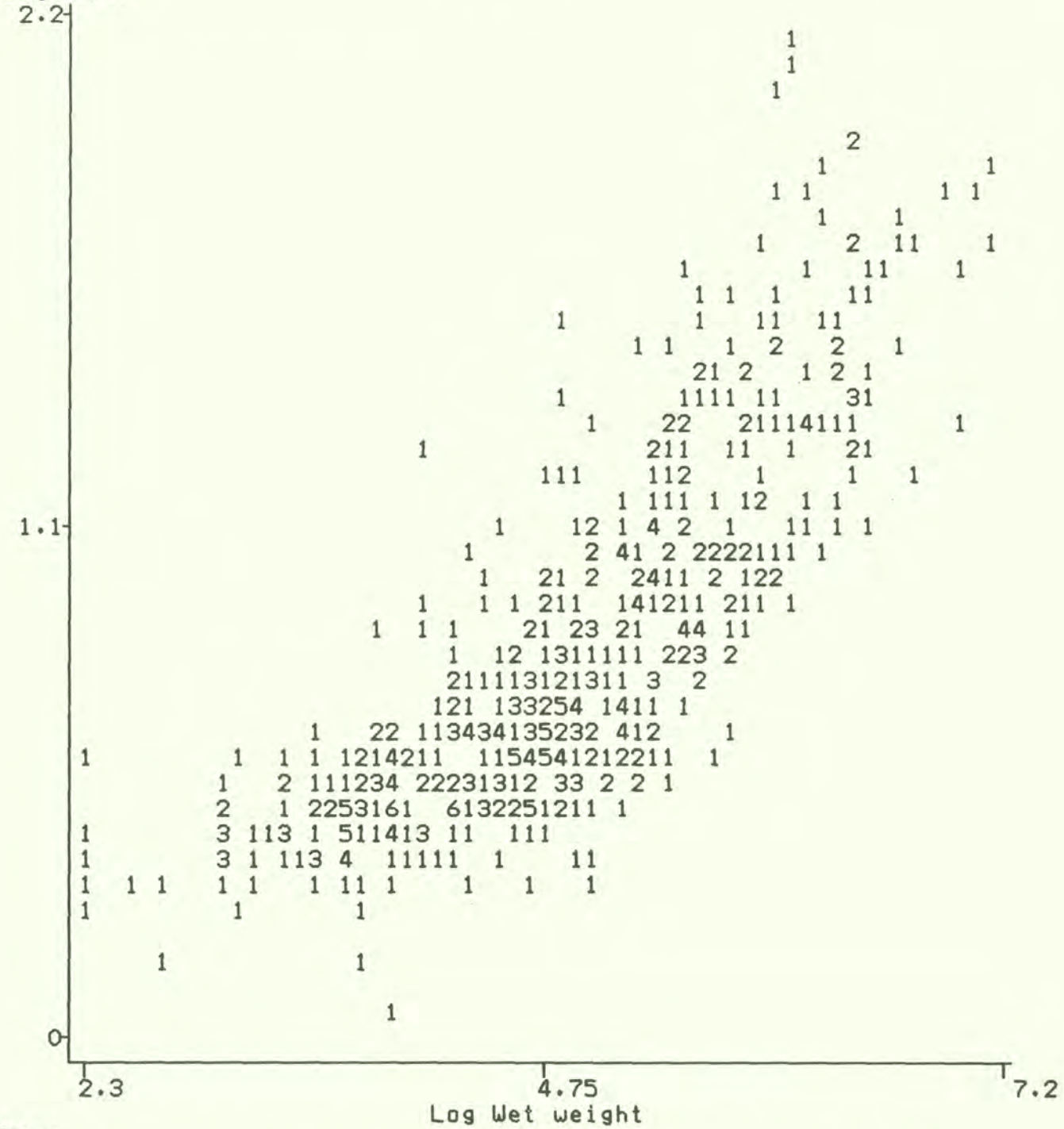

Key:

1=single data point in this row and column of the printer
2=two data share this location
3=three (etc)

Product-moment correlation coefficient
r = 0.803 d.f. = 542 t = 25.759 (p < 0.001)
Equation of major axis: y= .352 * x - .879

Figure 8: Correlation of (IR-R)/(IR+R) with Dry weight for all species.

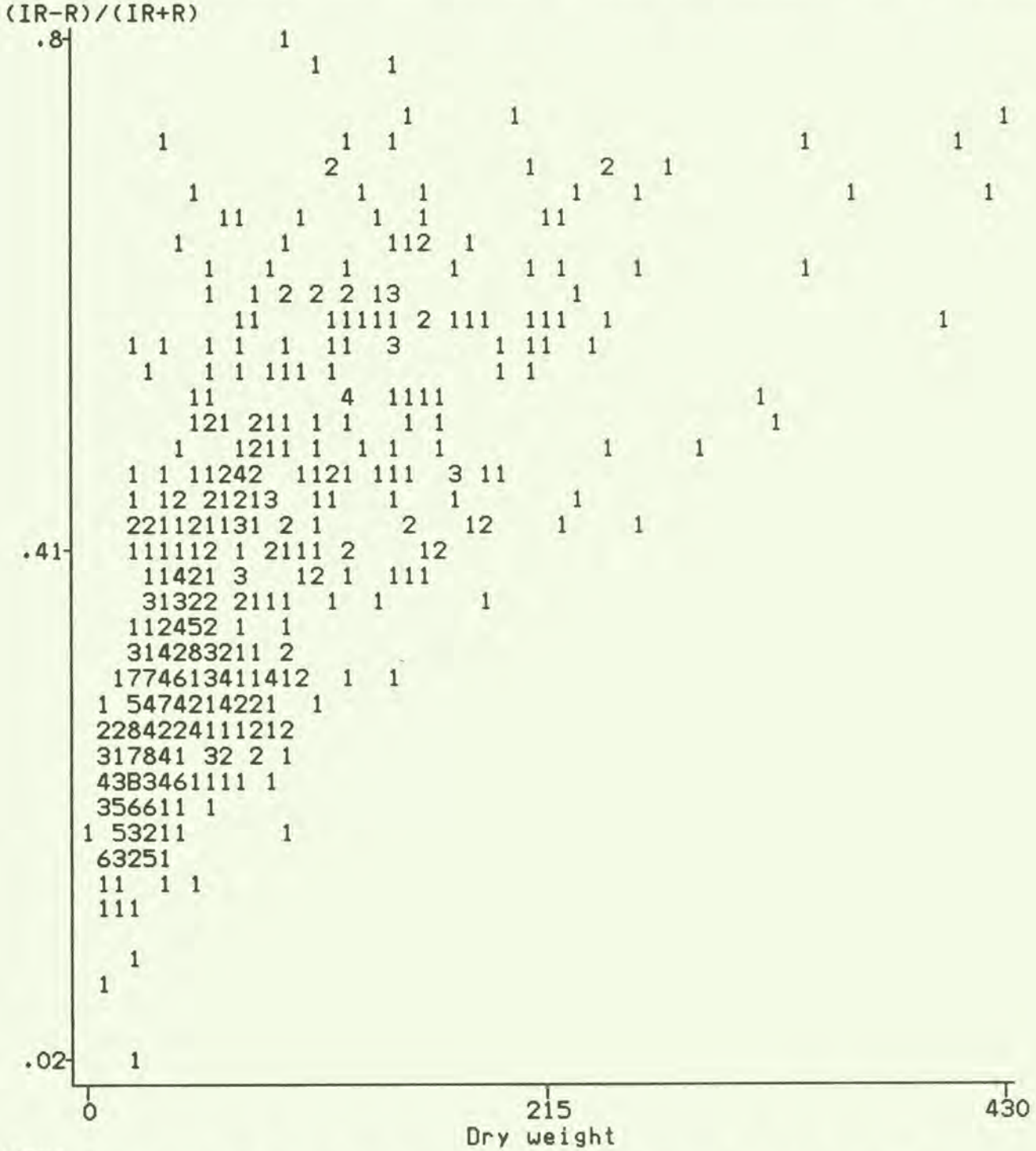

Key:

1=single data point in this row and column of the printer
2=two data share this location 3=three (etc)
A=ten data share this location B=eleven

Product-moment correlation coefficient
r = 0.694 d.f. = 542 t = 19.908 (p < 0.001)
Equation of major axis: y= .0015 * x + .267

Figure 9: Correlation of (IR-R)/(IR+R) with Log Wet weight for all species.

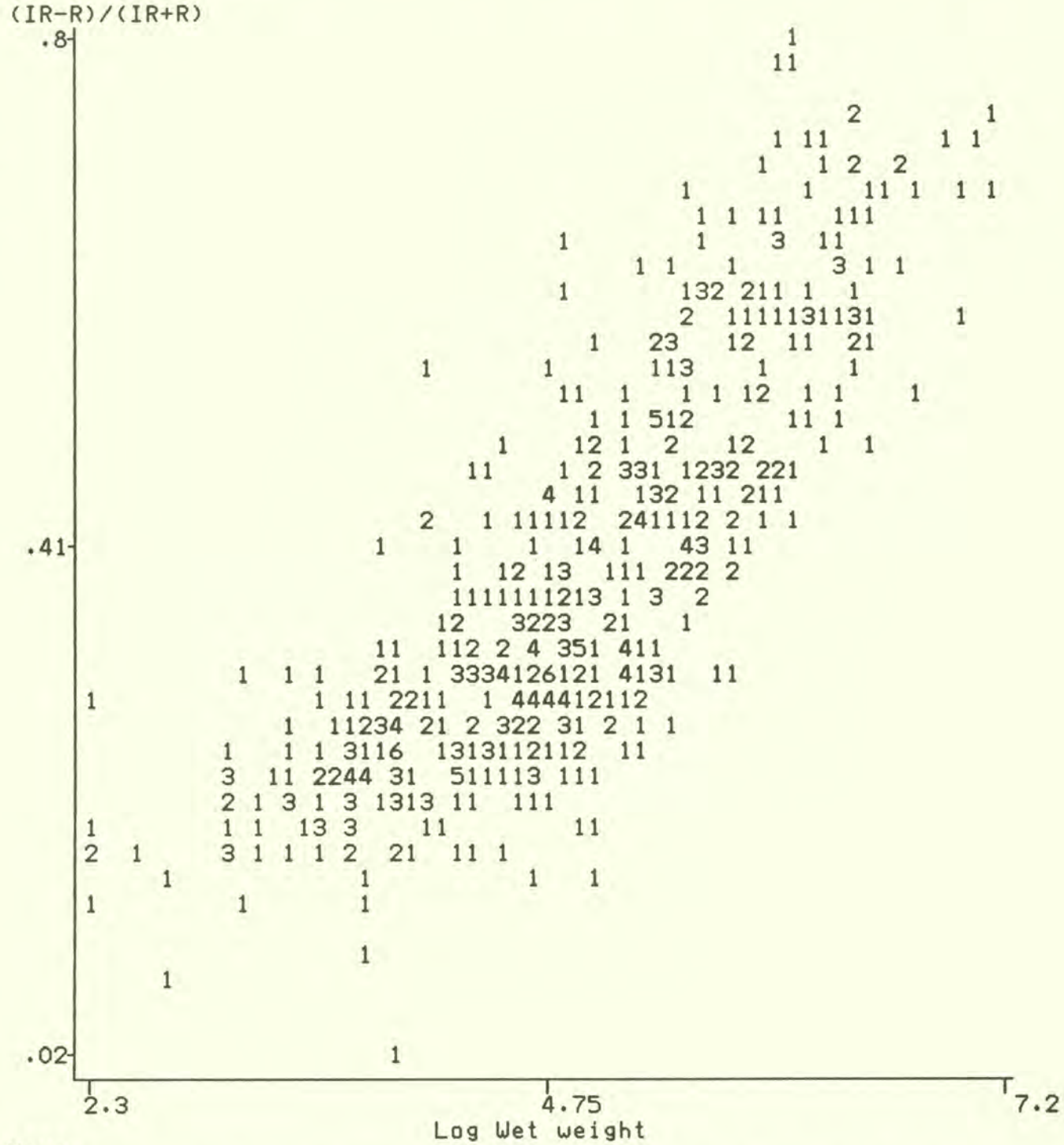

Key:
1=single data point in this row and column of the printer
2=two data share this location 3=three (etc)

Product-moment correlation coefficient
r = 0.819 d.f. = 542 t = 26.804 (p < 0.001)
Equation of major axis: y= .133 * x -.267

Table 5: R^2: Percent of variability explained by major axis of correlation of NDVI with biomass

Index	Wet wt	Log Wet wt	Dry wt	Log Dry wt
NDVI	60	67	48	54
log NDVI	49	64	42	54
√(NDVI+.5)	59	59	46	46

sample size=544

==========

Table 6: Mean dry biomass and 95% confidence limits estimated from four NDVI values.

NDVI	Estimated biomass (g/m^2)		
	Mean	95% confidence limits*	
		Lower	Upper
.25	19.3	7.7	114
.38	53.4	13.1	228
.52	159	28.0	431

*Confidence limits are taken from 95% confidence ellipse about data points

The estimate can be slightly, but not significantly, improved by using the square root transform of the NDVI, giving R^2=55% for the logarithm of dry weight and R^2=68% for that of wet weight.

Although the index correlates well with the logarithm of the dry weight, the spread of values of NDVI for any given biomass is considerable (Figure 10). Thus an area with a production of 55g/m² would "normally" be measured at an NDVI of 0.38, but the 95% confidence limits about this value are 0.14 and 0.63.

Conversely, the correlation of NDVI with log(dry weight) shows that, for any given NDVI, the estimated biomass may be a poor approximation of the actual biomass; thus Table 6 shows that with low values of the NDVI the true biomass may be six times greater than is the mean estimate (eg with an NDVI of .25 the upper 95% confidence limit is 114g/m² compared with the mean estimate of 19g/m²), while at high values of the NDVI the true biomass may be only a fifth or a sixth of the mean estimate (thus an NDVI of .52 corresponds to a mean biomass of 160g/m², but the lower 95% confidence limit is only 28g/m²).

6.9.6 Ratio of IR - R to the square root of IR + R (NDIST)

As an estimator of dry weight, wet weight and percent cover the index

$$\frac{IR-R}{\sqrt{(IR^2+R^2)}}$$

gave slightly (but not significantly) better correlations than did the NDVI. Careful comparison of Figures 10 and 11 will show that this improvement is brought about by a closer adherence of the outliers to the major axis at both low and high values of dry weight. In practical terms this means that incorrect predictions of biomass from radiometric data are likely to be slightly less inaccurate with the NDIST than they are with the NDVI.

The extra work involved in calculating this index relative to the NDVI is significant only for those analysts who do not have access to a computer or programmable calculator. Its use is nevertheless not recommended, firstly because the improvement over the NDVI is not significant, and secondly because the NDVI is widely used, and comparison of NDIST values with published NDVI values are likely to be inconvenient.

6.9.7 The Perpendicular Vegetation Index (PVI)

The PVI is measured in the plane formed by the infrared and red axes. It takes into account the observed linear relationship between IR and R measured over naked earth (Graetz 1985). The data collected in Senegal suggest that for naked earth,

Figure 10: Correlation of (IR-R)/(IR+R) with Log Dry weight for all species.

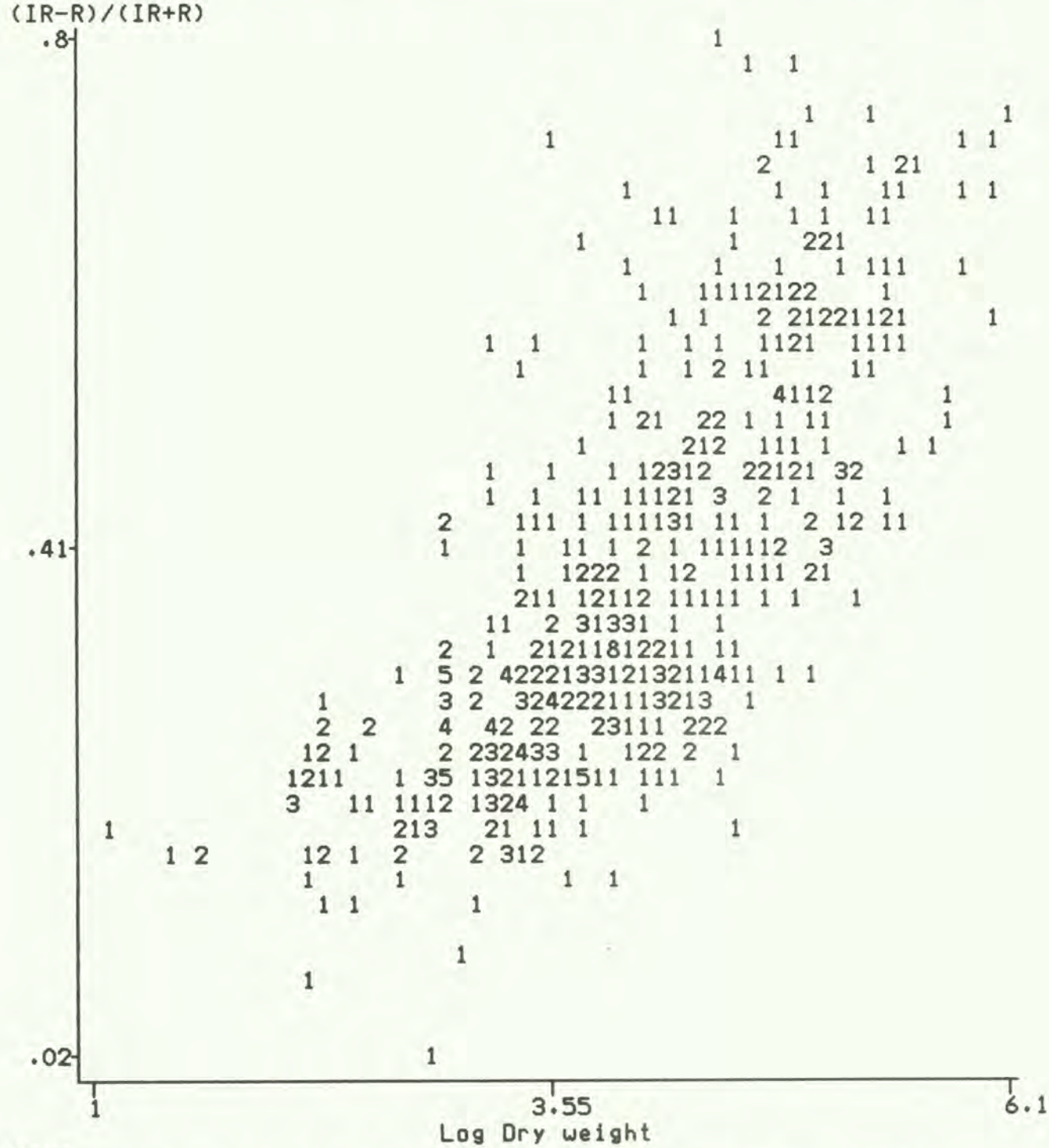

Key:
1=single data point in this row and column of the printer
2=two data share this location 3=three (etc)

Product-moment correlation coefficient
r = 0.737 d.f. = 542 t = 21.966 (p < 0.001)
Equation of major axis: y= .128 * x -.130

Figure 11: Correlation of $(IR-R)/\sqrt{(IR^2+R^2)}$ with Log Dry weight for all species.

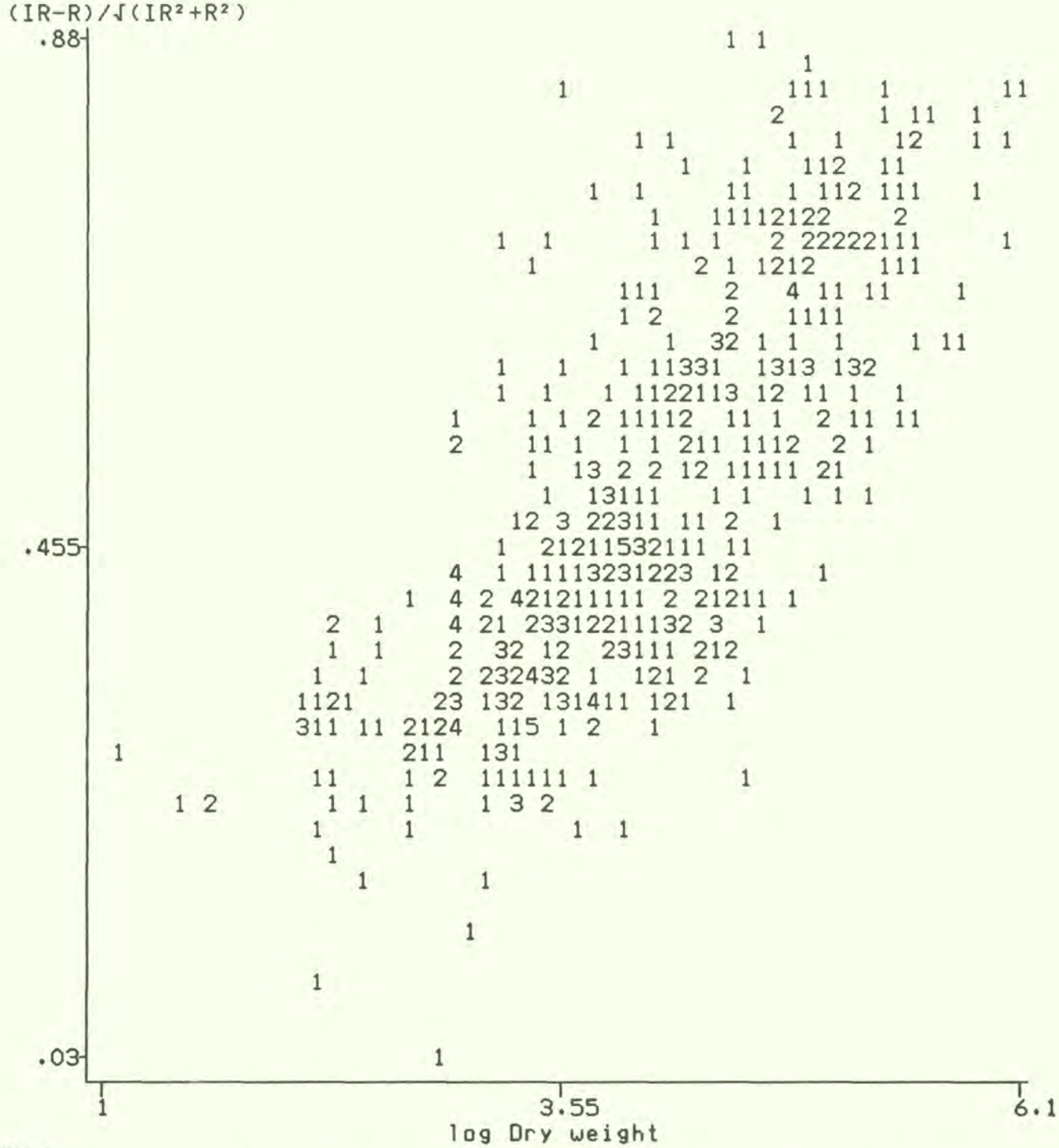

Key:
1=single data point in this row and column of the printer
2=two data share this location 3=three (etc)

Product-moment correlation coefficient
r = 0.748 d.f. = 542 t = 22.518 (p < 0.001)
Equation of major axis: y= .144 * x -0.082

$$\text{Infrared} = 0.91 * \text{Red} + 0.11 \qquad \text{(Section 6.9)}.$$

The PVI is then the perpendicular distance from this line to the point P whose coordinates are the values of infrared and red reflectance from the sample of vegetation.

In general, if d is the distance of the point (a,b) from the line whose equation is

$$y = mx + c$$

then

$$d = (b-ma-c)/\sqrt{(1+m^2)}$$

or in the specific case considered here,

$$PVI = \frac{(IR-0.91*R-0.11)}{\sqrt{(1+0.91^2)}}$$

This index gave poor results, being less accurate, and therefore less useful, than the simpler measure IR-R, to which, as can be seen by inspection of the formula, it is closely allied.

6.9.8 Other indices

Other combinations of IR and R were examined, but proved disappointing. It seems unlikely that any simple IR:R index will significantly improve on the NDVI, but radiometric estimates of biomass can be made considerably more accurate if the colour and especially moisture content of the background soil can be taken into account at the time of the measurement (Graetz 1984).

For the remainder of this report, only the NDVI is considered, although the analyses were all carried out with other indices as well. The results of the unpublished analyses are in the safekeeping of GEMS.

Table 7 shows the five indices whose correlations with dry weight, wet weight and percent cover were greatest.

6.10 Improvements by considering species composition

Since the species composition of the plots used to collect the data was recorded, it is possible to examine the efficiency of radiometric measurement on pure (that is, single-species) stands or stands having given species characteristics.

Only four graminaceous species (Aristida mutabilis, Cenchrus biflorus, Chloris prieurii and Schoenefeldia gracilis) and one non-graminaceous species (Zornia glochidiata) were present in the grass-layer samples sufficiently often (N>=30) for reliable results to be obtained on stands dominated by these species, and only two (Aristida mutabilis and Chloris prieurii) were present sufficiently often as pure stands.

Table 7: Indices whose correlations with dry weight, wet weight and percent cover were greatest

Log Dry weight	
Index	Corr
Log volume	.846
$(IR-R)/\sqrt{(IR^2+R^2)}$	.748
$\sqrt{((IR-R)/(IR+R)+.5)}$	.743
$(IR-R)/(IR+R)$	.737
$Log((IR-R)/(IR+R))$	.735

Log Wet weight	
Index	Corr
$(IR-R)/\sqrt{(IR^2+R^2)}$	.825
$\sqrt{((IR-R)/(IR+R)+.5)}$	.823
$(IR-R)/(IR+R)$	.819
Log volume	.813
$Log((IR-R)/(IR+R))$	.803

Arcsine Percent Cover	
Index	Corr
$\sqrt{((IR-R)/(IR+R)+.5)}$	.711
$(IR-R)/\sqrt{(IR^2+R^2)}$	.711
$(IR-R)/(IR+R)$	.709
$Log((IR-R)/(IR+R))$	.707

6.10.1 Radiometric response of pure stands

The slopes of the major axes of the correlation between the NDVI and the biomass of pure stands of Aristida mutabilis and Chloris prieurii were near 0.13 (Table 8), irrespective of whether wet or dry weight was considered. The intercepts for wet weights for these two species were similar, at about -0.27, but apparently differed from those of dry weights for the same species (roughly -.18), so that the calibration curves for wet and dry weights would be parallel but have different elevations.

The slope and elevation of the major axes for the correlation between NDVI and percent cover for these two species are apparently different (Table 8), with the slope for Aristida mutabilis being about 1.5 times that for Chloris prieurii. This may be a result of their different growth forms. More research should be done before coming to any firm conclusion, since these results, based on small sample sizes (near 40) exhibit considerable variability around the major axis.

6.10.2 Stands of graminaceous species

The NDVI responded more sensitively (steeper slope) to increases in dry weight than it did to increases in the wet weight of stands of graminaceous species dominated by Aristida mutabilis, Chloris prieurii and Schoenefeldia gracilis. However, there seems to be no generality in this observation since stands of graminaceous species dominated by Cenchrus biflorus showed the opposite radiometric behaviour (Table 8), and the slope of the major axis varied from about 0.13 to about 0.19 (NDVI against the logarithm of the wet weight).

The dominant species therefore seems slightly to influence the measure of NDVI for a given biomass. It also seems possible that the quality of the grasses may influence the NDVI. Boudet's (1983) classification of grass-layer forrage plants was used to select samples in which the dominant and subdominant plant species belonged either to

- Class 1: medium to tall tillering grasses, palatable to livestock in both green and dry state,

- Class 2: small to medium grasses with thin tough stems, palatable when green but less so when dry,

or

- Class 3: small grasses with tough stems and few leaves.

Results are presented in Table 9, from which it may be seen that the NDVI is more sensitive to changes in weight of stands of Class 1 plants than it is to changes in weight of stands of Class 2 or 3 plants.

6.10.3 Stands of non-graminaceous species

Table 8: Slopes and elevations of major axis of correlation between production parameter and NDVI

	Aristida mutabilis		Cenchrus biflorus		Chloris prieurii		Schoenefeldia gracilis	
	slope	icpt	slope	icpt	slope	icpt	slope	icpt
PURE STAND								
A/sin Cover	.560	.022			.382	.087		
Log(Wet wt)	.132	-.287			.127	-.250		
Log(Dry wt)	.130	-.192			.131	-.172		
GRAMINACEOUS SUBDOMINANTS								
A/sin Cover	.469	.079			.407	.099	.593	.035
Log(Wet wt)	.141	-.338	.187	-.590	.125	-.254	.168	-.467
Log(Dry wt)	.149	-.259	.159	-.280	.131	-.179	.194	-.445
ANY SUBDOMINANTS								
A/sin Cover	.476	.070	.564	.059	.445	.088	.374	.152
Log(Wet wt)	.138	-.313	.147	-.353	.114	-.192	.145	-.343
Log(Dry wt)	.147	-.242	.118	-.077	.129	-.163	.163	-.312

	Zornia glochidiata	
	Slope	Intercept
NON-GRAMINACEOUS SUBDOMINANTS		
A/sin Cover	.446	.169
Log(Wet wt)	.169	-.368
Log(Dry wt)	.129	-.046
ANY SUBDOMINANTS		
A/sin Cover	.425	.172
Log(Wet wt)	.169	-.358
Log(Dry wt)	.150	-.104

Note: (1) "icpt" is the intercept of the major axis with the axis representing the radiometric index

(2) "A/sin Cover" is the Arcsine of the proportion of ground covered by the vertical projection of the aerial parts of the vegetation in the plot.

Table 9: Slopes and elevations of major axis of correlation between production parameter and NDVI for all graminaceous stands

	Class 1		Class 2+3		All		>=30% water	
	slope	icpt	slope	icpt	slope	icpt	slope	icpt
A/sin Cover	.580	.028	.458	.092	.481	.081	.492	.080
Log(Wet wt)	.136	-.303	.117	-.212	.132	-.288	.139	-.326
Log(Dry wt)	.143	-.218	.110	-.098	.137	-.200	.140	-.208

Note: (1) "icpt" is the intercept of the major axis with the axis representing the value of the radiometric index

(2) "A/sin Cover" is the Arcsine of the proportion of ground covered by the vertical projection of the aerial parts of the vegetation in the plot.

Stands of non-graminaceous species dominated by Zornia glochidiata behaved radiometrically as did stands of graminaceous species dominated by Cenchrus biflorus, except that increases in wet or dry weight led to smaller increases in NDVI (Table 8).

6.10.4 Water content of stands

Fewer than 10% of the stands characterised by graminaceous dominants and subdominants had less than 30% water content. In a correlation restricted to those samples for which water content was greater than 30%, the NDVI was slightly more sensitive to changes in weight (Table 9). Although the increase in sensitivity was probably not statistically significant, the result cannot refute the hypothesis that the proportion of water in the plants changes the sensitivity of the index to changes in weight.

This observation is likely to be of little significance for practical work in the Sahel, since the exact phenological stage of any one stand is out of the observer's control. There will be a restricted period near the end of the growing season for which the radiometer will be used to estimate maximum production, and the erratic variation from site to site in the vegetative cycle will prevent the observer from determining water content until after the sample has been clipped and weighed. Clearly, if the sample is to be clipped there is normally little to be gained by using the radiometer.

Lamprey and de Leeuw (1986) found a statistically highly significant relationship between NDVI and the percent cover multiplied by the ratio between wet and dry weight, which they consider to imply that water content is proportional to chlorophyll activity. On the face of it, the data from Senegal apparently tend to support their finding (if not their conclusion); the relationship % Cover * W/D accounts for 50% of the variability in NDVI. However, the correlation between NDVI and % Cover alone is at least as good (r=0.709 for NDVI and % Cover; r=0.704 for NDVI and % Cover * W/D): the inclusion of W/D is at best neutral.

6.11 Naked earth

In order to investigate the variability of the contribution to the radiometric measures of the background to the vegetation, 40 measurements of the radiometric response of naked earth were collected at different sites on a 130km north-south transect between 8h30 and 16h45 on a single day in July. The soils on the transect were principally yellowish grey and sandy. No measures of soil moisture content were made. The normalised difference

$$(IR-R)/(IR+R)$$

remained remarkably constant at 0,277+/-0,019. No relationship between the value of the index for naked earth and time of day was noted (Table 10), except that there seemed to be a tendency towards increasing

Table 10: Radiometric measurements on naked earth 12 July 1984

Time	Approximate Red	Approximate Infra-Red	ND
8.32	3.88	6.93	.28
8.33	4.04	7.02	.26
8.36	4.38	7.67	.27
8.41	4.81	8.71	.28
9.28	6.25	11.5	.29
9.30	6.28	11.0	.27
9.32	6.83	12.5	.29
9.33	6.97	12.3	.27
9.33	6.89	12.3	.28
9.35	7.07	12.3	.27
9.37	6.96	12.6	.28
9.38	7.04	12.5	.27
9.41	9.30	15.7	.25
9.59	7.97	13.8	.26
10.01	7.69	13.8	.28
10.01	7.19	13.0	.28
10.03	7.76	14.2	.29
10.04	6.81	12.3	.28
10.29	9.54	17.2	.28
10.30	8.84	15.6	.27
10.31	9.55	17.2	.28
10.32	9.53	17.2	.28
10.34	9.55	16.9	.27
11.27	11.6	20.9	.28
11.28	11.9	21.3	.28
11.36	14.2	24.4	.26
11.37	13.2	21.9	.24
11.38	13.4	22.4	.25
11.39	15.0	24.6	.24
11.50	11.2	21.0	.30
12.18	9.95	17.4	.27
12.19	12.2	22.2	.29
12.21	12.8	22.4	.27
12.43	12.8	23.1	.28
12.46	12.8	23.1	.28
13.08	13.4	23.9	.28
15.50	6.86	12.4	.28
15.50	7.24	14.0	.31
16.33	5.16	10.8	.35
16.46	5.34	9.89	.29

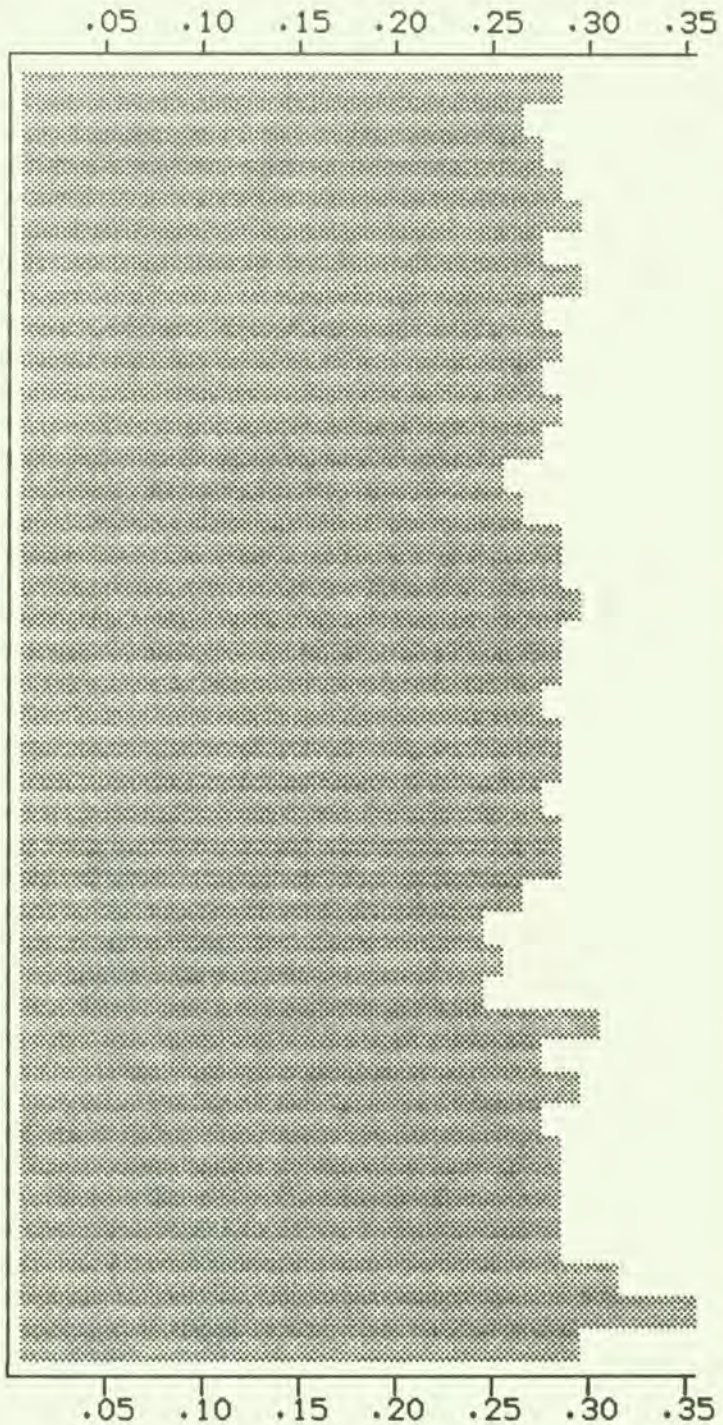

Summary Statistics:

sample size = 40
mean normalized difference = 0.277
standard deviation of normalized difference = 0.0186
as percentage of mean = 6.70%
minimum normalized difference = 0.24
maximum normalized difference = 0.35

variability in the NDVI in the later part of the afternoon. Given the experimental conditions, it is of course impossible to say whether this tendency arises from some effect of time of day or changes in soil type or moisture.

7 The air-borne instrument

The Pilot Project for the Inventory and Monitoring of Sahelian Pastoral Ecosystems was unable to test the radiometer mounted in an aircraft.

Initial experiments in Kenya (Lamprey and de Leeuw 1986) have shown that, provided that the vegetation is green, the NDVI is correlated with the proportion of the ground covered by vegetation, as estimated from aerial photographs taken at the same time as the radiometer readings. They go on to show that NDVI is even more strongly correlated with the percent cover multiplied by the greenness of the vegetation estimated from colour photographs. From their data it can be deduced that the correlation between (cover * greenness) and (dry weight) is highly significant ($r=0.97$; $n=20$), and hence that properly calibrated airborne radiometers can be used to estimate biomass. A probable application for this is to use the airborne radiometer to calibrate data collected by satellite-borne instruments.

However, it is evident from their data that a visual estimate (cover * greenness) gives a better estimate of standing green biomass than does the NDVI.

8 The satellite borne instrument

Radiometers carried in satellites, and some of those carried in aircraft, build up a record of the radiation from an area of the earth's surface by detecting and recording the radiation from one limited part of the scene after another. The fraction of the scene, or picture element (from whence the word "pixel" was coined), is represented by a single value in whatever wavelength is being detected, and is therefore in some sense an average value of the intensity of radiation from the various surfaces within that part of the scene. The resulting image is thus composed of row after row of aligned pixels. (The principle of the Return Beam Vidicon carried on board the first Landsat satellites was different; in this instrument the image was first recorded on a photosensitive surface and this surface was then scanned by an electron beam.)

The manner in which the scene is scanned varies from instrument to instrument: some use a rotating or rocking prism or mirror to deflect radiation from successive parts of the scene to the sensor, while others (notably SPOT's High Resolution Visible Imaging Instrument) use a battery of radiometrically identical and precisely aligned sensors aimed at different parts of the scene. (The action of SPOT's instrument also involves mirrors, but they are used to collect radiation coming from parts of the earth's surface that happen to be off nadir at the time of passage of the satellite.)

The scanning radiometer itself does not normally produce an image, and indeed for most analyses carried out on the data captured by a radiometer it is preferable to leave the information in the digital form in which it is recorded (or, in the case of satellite data, transmitted to the earth receiving station). The digital data are then processed by computer, and, after treatment, may be provided to the user in the form of graphs, histograms, tables or density-sliced, coloured images.

8.1 Requirements of spatial and temporal resolution in ecological monitoring

The growing season in the Sahel is from two to three months long, and in some cases significant spurts of growth can start and end in less than 20 days (Tucker et al 1985). Without frequent data aquisition it may be impossible to follow important developments in the pastures. The Sahel is a very large area and a general view of many tens or hundreds of thousands of square kilometers is frequently required.

Under these circumstances the satellite must be in a position for the instrument to collect data at short intervals, of the order of a few days, but the on-board radiometer need not be capable of a particularly high resolution. The AVHRR on board NOAA satellites fills these criteria better than any other current orbital radiometer (Table 11), and its data were therefore used by the Project to test the possibility of monitoring primary production in the Sahel using an orbital radiometer.

8.2 Presentation of uncalibrated data

The data received by the Project were in the form of colour transparencies or Polaroid prints of the NDVI derived from the AVHRR, colour coded so that a given range of NDVI was represented by a unique colour. Since the data were not in digital form the biomass samples could not be compared directly with the NDVI calculated from the reflectances measured from the pixel concerned.

In the images consisered here, the NDVI values were derived from data collected on several dates during the growing season. The value assigned to any one pixel was calculated by a polygon integration of its successive values on the different dates. The success of this integration depends on the accuracy with which the successive images are registered to one another. The technique used was to register each image to the coastline of Africa by eye.

8.3 Sample distribution

The centroid of the samples collected over 4 years was at N16°03' W14°57'. Of the 249 samples, only about 30% were collected to the south of the centroid of the field area, at N15°55' W14°39'. Since there is a strong north-south rainfall gradient in the area (GEMS 1986b), wetter,

Table 11: Characteristics of various important earth-resources satellites and their on-board radiometers

Satellite	Alti-tude (km)	Orbit (min)	Retn time (dy)	Radio-meter	N	Ch No	Spectral Range (μm)	Swath Width (km)	Pixel size (m)
Landsat 1-2	918	104	18	MSS	4	4	0.5 -0.6	185	56x79
						5	0.6 -0.7		
						6	0.7 -0.8		
						7	0.8 -1.1		
				RBV	3		0.48-0.58	185	79
							0.58-0.68		
							0.70-0.83		
Landsat 3	see Landsat 1-2, except:			RBV	2		0.51-0.75	99	24
Landsat 4-5	705	98.9	16	MSS	<------ as Landsat 1-3 ------>				
				TM	7	1	0.45-0.52		30
						2	0.52-0.60		30
						3	0.63-0.69		30
						4	0.76-0.90		30
						5	1.55-1.75		30
						6	10.4-12.5		120
						7	2.08-2.35		30
TIROS-N NOAA 6-8	833-870	102	9.2	AVHRR		1	0.55-0.68	2800	1100
						2	0.73-1.10		
						3	3.55-3.93		
						4	10.5-11.5		
NOAA-7						5	11.5-12.5		
SPOT	832	101	26	HRVms*			0.50-0.59	60	20
							0.61-0.68		
							0.79-0.89		
				HRVpc*			0.51-0.73	60	10

*HRVms = High Resolution Visible radiometer in multispectral mode
HRVpc = High Resolution Visible radiometer in panchromatic mode

more productive areas of the zone were under-sampled. More than 70% were collected to the east of the central meridian of the field area (Figure 12). This sample distribution corresponds roughly to the distribution of firebreaks, which are more dense in the north-western, sandy quarter of the area than in the south eastern, gravelly quarter.

The median weight of the biomass sampled represented 375 kg/ha (interquartile range from 214 to 744 kg/ha). As can be inferred from the interquartile range, the frequency distribution was strongly skewed (Figure 13).

8.4 Treatment of the data

Samples were collected in the field in such a way that not all of the colours represented on the images could be assigned a corresponding value of biomass. By pooling colours representing adjacent ranges of NDVI values, eight classes were derived and used in the analyses. These eight classes covered a range of NDVIs from 0.01 to 0.25.

The proportion of the field area categorised into the various classes varied greatly from year to year (Table 12). Averaged over the four years, class 1, representing the lowest range of NDVI values and productivity, covered a mean of 29% of the field area. Classes 2 through 8 covered roughly 14%, 12%, 9%, 12%, 10%, 10% and 5% of the field area respectively. Because of the way in which the samples were collected, the three classes of lowest productivity were over-sampled, with 28%, 21% and 17% of the sampling effort respectively, and the five highest classes were under-sampled by comparison with their relative areas in the field.

Previous work (Vanpraet et al 1983) used NDVI values derived retroactively from the colour scale of the images. This may have given the impression that digital values were available; this report depends on the pooled classes.

8.5 Results

Over the range of biomass sampled by the Project, a linear relation could be assumed between the median biomass in a class and the NDVI derived from the satellite AVHRR data (Vanpraet et al 1983). However, the spread of values of NDVI for any given biomass is large (Figure 14a). Samples of biomass estimated between about 500 kg/ha and 800 kg/ha were on different occasions classified into each of the 8 classes.

Furthermore, the means and interquartile ranges of dry biomass in the eight classes (Figure 14b) show that class 8 and class 5 seem to be misplaced relative to classes 7 and 4 respectively. The number of classes was therefore reduced to 6 by pooling classes 8 and 7 and classes 5 and 4. Reanalysis of the means and interquartile ranges (Figure 15) now suggests a curvilinear relationship of NDVI class with dry biomass, and by plotting the NDVI class against the log of the biomass (Figure 16a and b) a linear relationship between the two variables is found.

Figure 12: Distribution of field samples of biomass collected in 1980-1983 for the calibration of AVHRR images

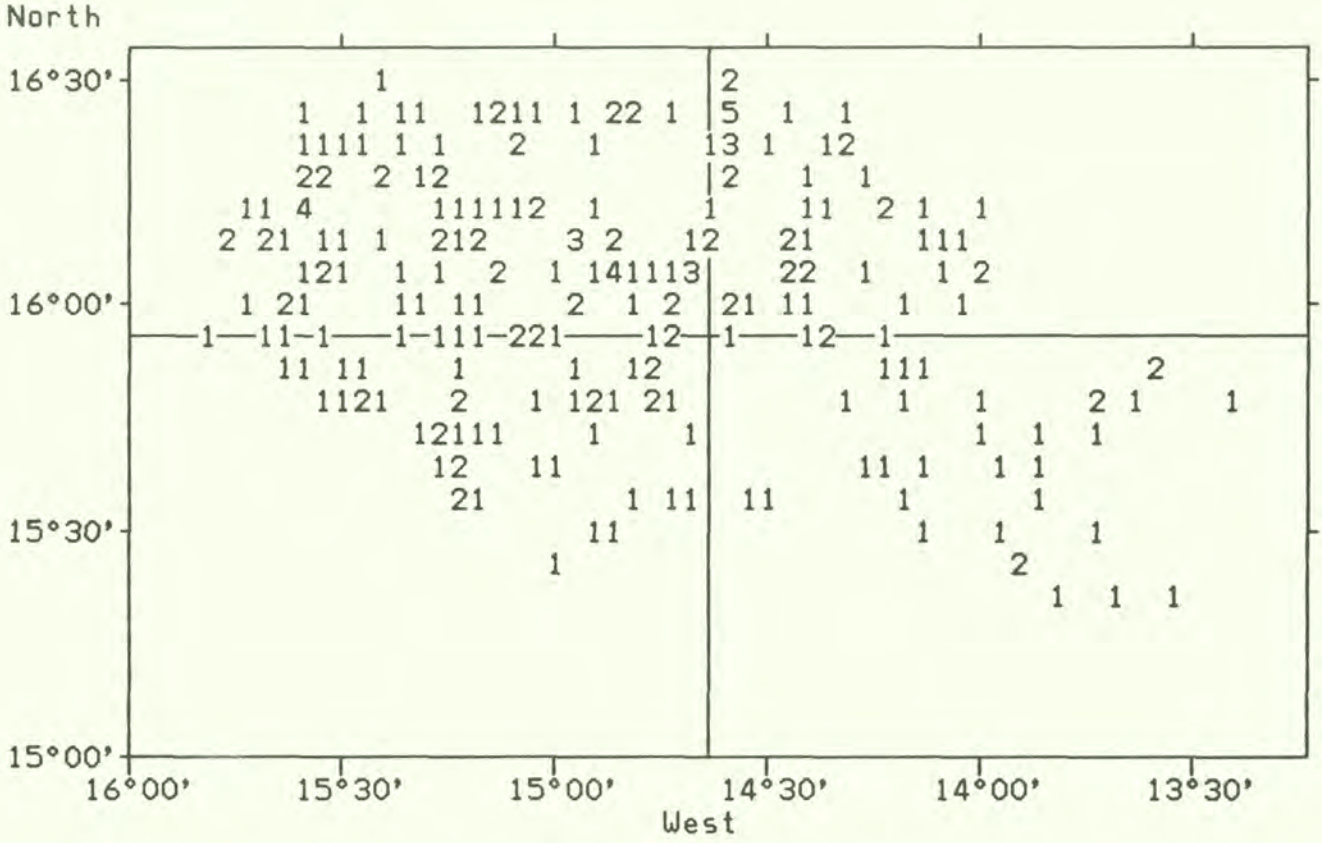

The cross through the centre of the diagram marks the centroid of the field area.

Figure 13: Frequency distribution of dry weight of samples collected for calibration of AVHRR images

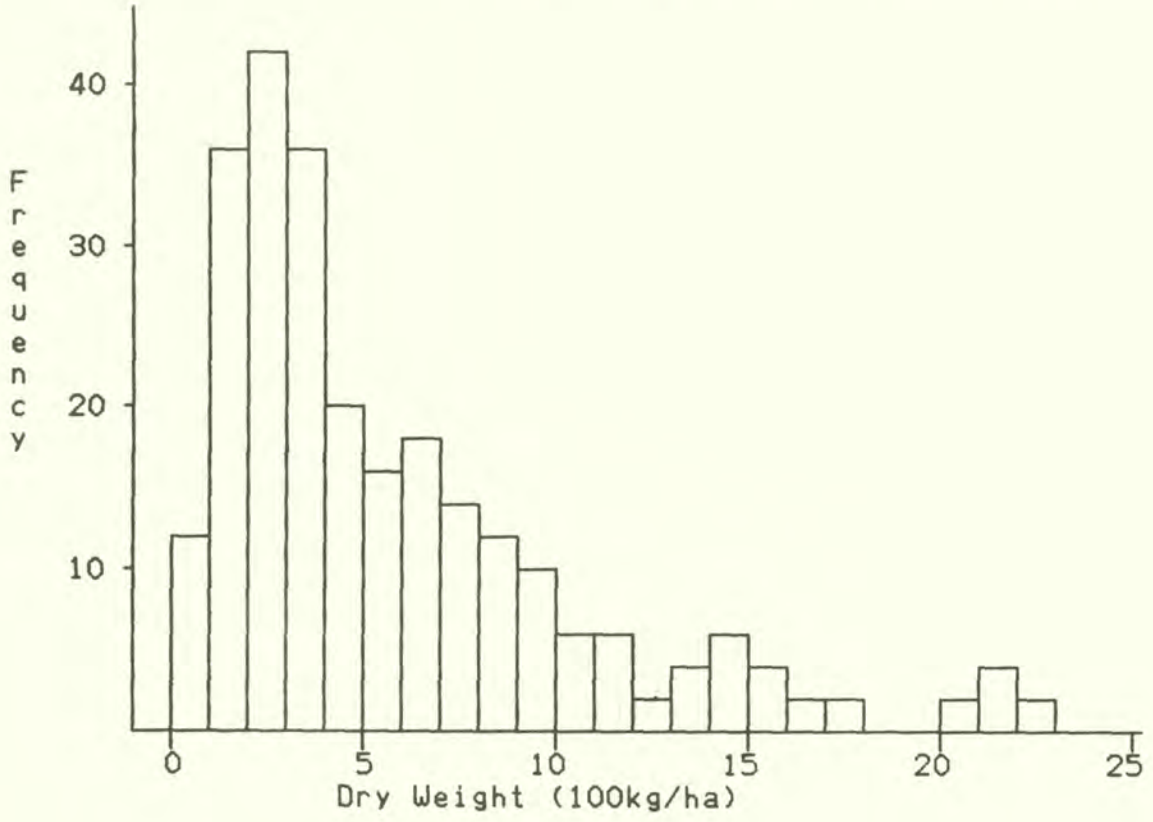

Table 12: Estimates* of proportion of field area covered by each of 8 classes of NDVI values

Class	1980	1981	1982	1983	Mean
1	17.5	1.6	19.3	77.2	29.0
2	16.4	7.0	14.4	17.5	13.8
3	13.2	4.3	27.3	3.2	12.0
4	11.6	14.4	8.6	0.5	8.8
5	14.8	13.9	16.6	1.6	11.7
6	12.2	13.4	13.9	0.0	9.8
7	5.8	33.2	0.0	0.0	9.7
8	8.5	12.3	0.0	0.0	5.2

*Proportions were estimated from a systematic random sample of 200 points on each image. Binomial 95% confidence limits are generally of the order of ±5%.

==========

Table 13: Annual correlations of NDVI class with dry weight and latitude

	Dry weight		Latitude	
	r	probability	r	probability
1980	0.207	ns	-.632	<.001
1981	0.635	<.001	-.729	<.001
1982	0.653	<.001	-.763	<.001
1983	0.558	<.001	0.090	ns

==========

Table 14: Approximate values of biomass (kg/ha) represented by coloured areas on AVHRR NDVI images 1980-1983

Class	Median	Interquartiles		Suggested Values for Key (kg/ha)
		Lower	Upper	
1	200	130	300	0-220
2	250	150	400	220-370
3	420	340	670	370-550
4	620	460	900	550-840
5	970	770	1410	840-1200
6	1310	970	1640	>1200

Figure 14a: Correlation of NDVI class with dry weight (kg/ha) for 1980-1983: eight classes

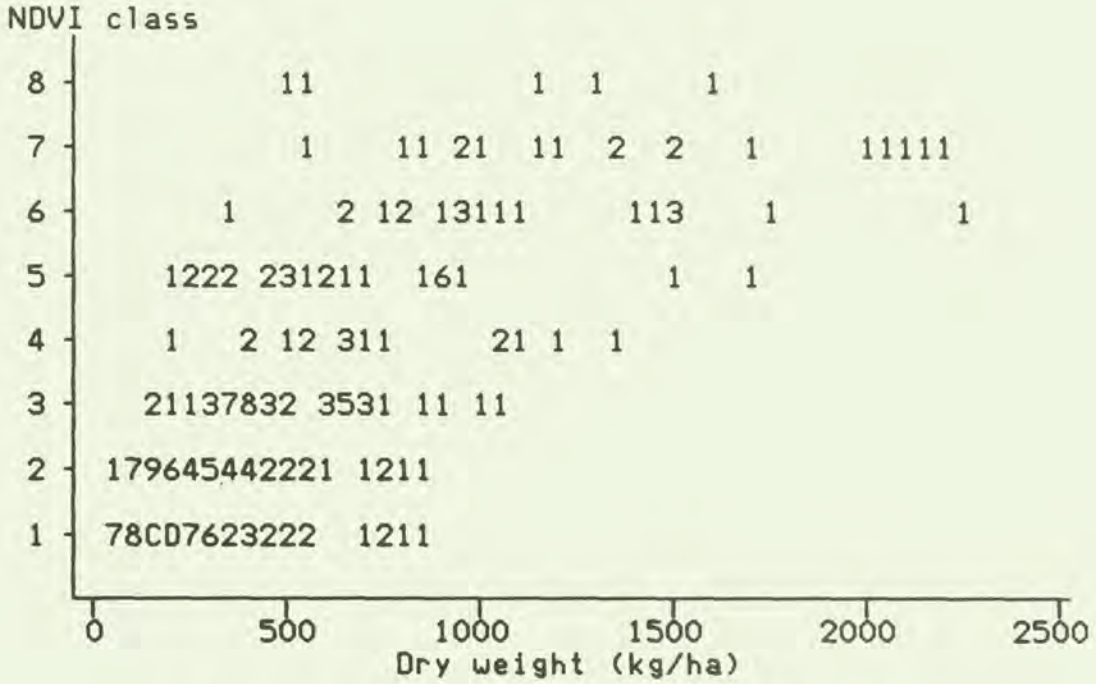

Product-moment correlation coefficient
r = 0.731 d.f. = 248 t = 14.615 ($p < 0.001$)
Equation of major axis: NDVI = .0033 * Dry Wt + 1.35

==========

Figure 14b: Correlation of NDVI class with dry weight (kg/ha): medians and interquartile ranges for eight classes 1980-1983

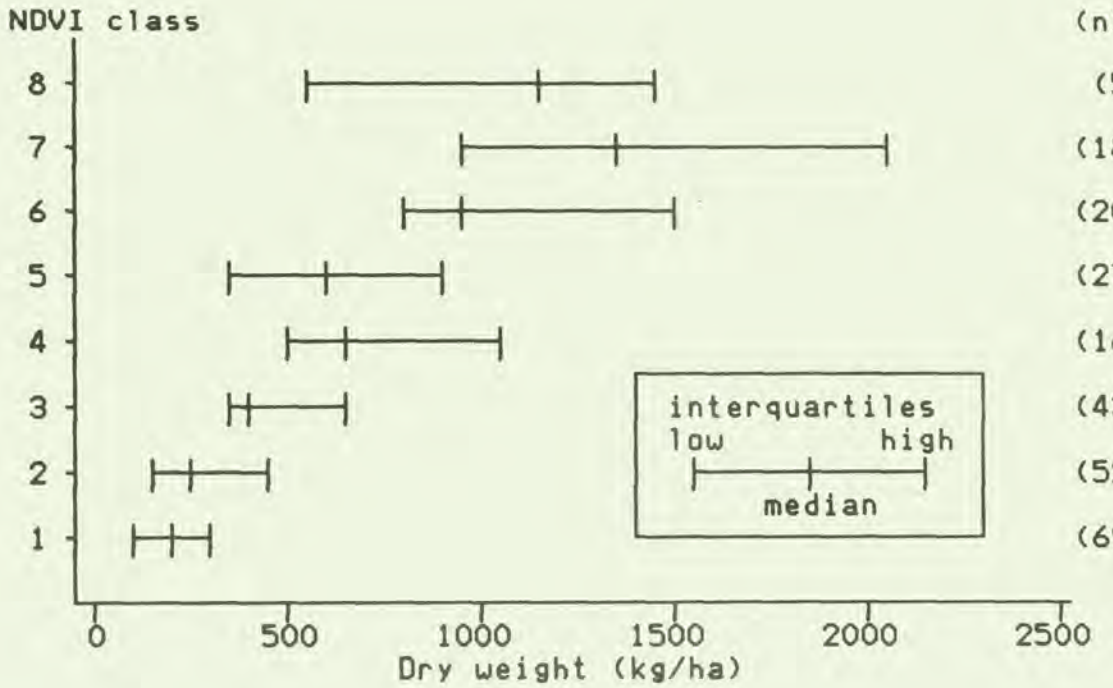

Figure 15: Correlation of NDVI class with dry weight (kg/ha): medians and interquartile ranges for six classes 1980-1983

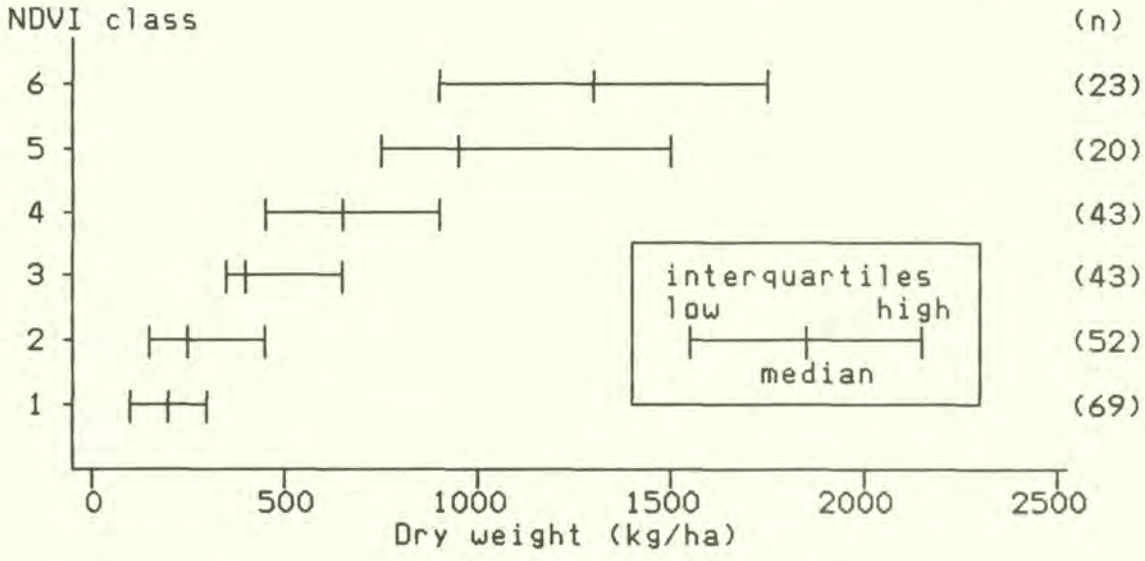

Product-moment correlation coefficient
r = 0.734 d.f. = 248 t = 14.735 ($p < 0.001$)
Equation of major axis: NDVI= .0026 * Dry Wt + 1.42

Figure 16a: Correlation of NDVI class with logarithm of dry weight for 1980-1983: six classes

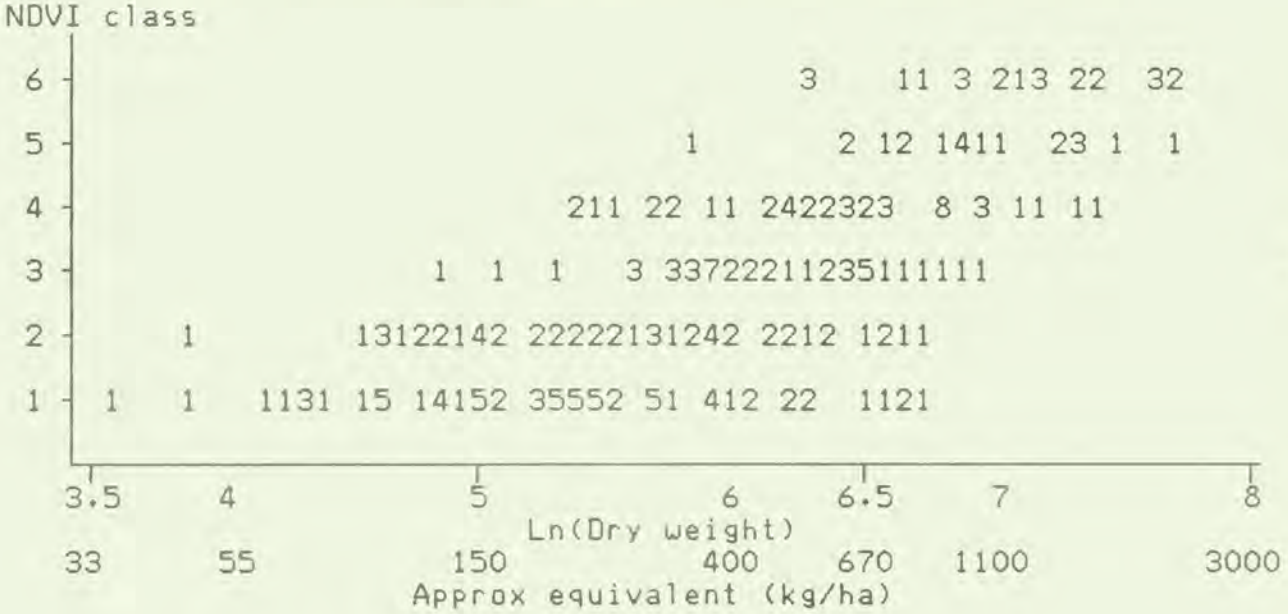

Product-moment correlation coefficient
r = 0.727 d.f. = 248 t = 14.492 (p < 0.001)
Equation of major axis: NDVI = 2.34 * ln(Dry Wt) -11.14

==========

Figure 16b: Correlation of NDVI class with dry weight (kg/ha): medians and interquartile ranges for six classes 1980-1983

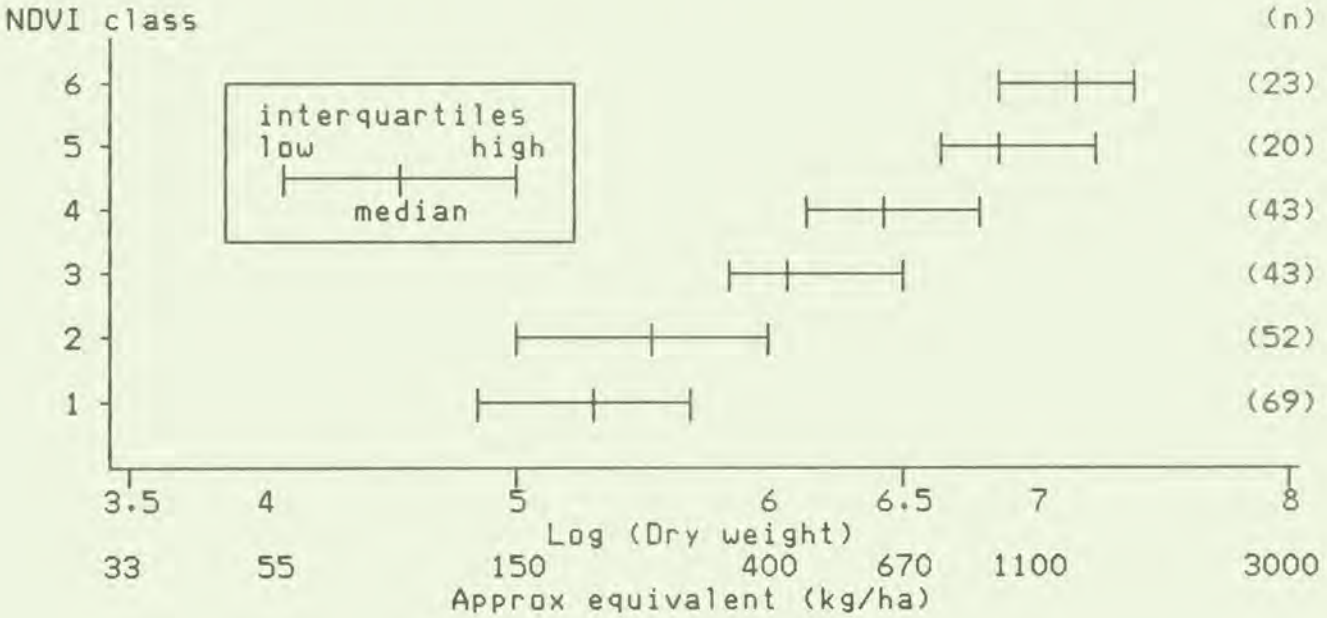

It will be observed that the correlation coefficient of ln(Dry Wt) against NDVI class (Figure 16a) is slightly poorer than that for the linear correlation (Figure 15), because of the greatly increased relative spread of biomass in the low classes. This is not evident in the plot of means and interquartile ranges (Figure 16b), although there is still considerable overlap between the classes.

Correlations between the NDVI class and dry biomass for the data collected for each year taken individually were high in 1981, 1982 and 1983 (Table 13), but very poor in 1980.

In 1980, 1981 and 1982 the NDVI class was more highly correlated with latitude than it was with biomass, although in 1983, a year of disastrously poor primary production, the north-south gradient of classes was not evident.

8.6 Calibration of the images

From the point of view of the scientist interested in the technique of radiometry for the estimation of standing fodder biomass in the Sahel, calibration of the images would be best achieved by presenting Figure 16b, appropriately coded to correspond with the corresponding colours, with the published image.

In order to provide a key more acceptable to range ecologists and governmental offices, the upper and lower interquartile limits of adjacent classes could be summed and divided by 2, giving the approximate limits to the classes on the map (Table 14).

8.7 Preparation and presentation of satellite data

The Project prepared outline maps at a scale of 1:500000 and then projected the image onto them using a slide projector, an overhead projector or an optical pantograph to enlarge the original image. The instrument used depended on the presentation of the image received from NASA.

The River Senegal, which is made up of multiple braided streams, occupies a wide shallow bed from 10 to 30km across. This relatively productive tract stands out clearly against the less productive surrounding lands on the satellite images. The Lac de Guiers is also clearly visible.

The image was registered by overlapping the representations of the river and the lake on their representations on the outline map. A limited amount of geometric correction could be introduced by altering the angles of the projector and screen. The lines enclosing blocks of each colour were then traced by hand onto the outline map.

The sites of the biomass samples were then located on the resulting prototype map. Their distribution determined the way in which colour-

slices were pooled, and their values were used to calibrate the remaining density slices. A fair copy of the preliminary map was prepared and duplicated, and the resulting maps were then coloured by hand and delivered to the interested Government agencies. They were accompanied by a note giving details of species composition of the pastures and warnings of fire risk in any threatened areas, that is, all areas with more than 700 kg/ha. Reproductions of these maps, redrawn at roughly 1:2000000, are included in this report (Figures 17 to 19).

8.8 The biomass maps of 1980-84

The salient feature of these maps, taken together, is the great difference in production detectable from year to year, and specifically the outstandingly poor production in 1983 and 1984. In 1984, particularly, only an insignificant fraction of the test zone produced more than 200kg/ha. In effect, for two years the pastoral economy of the area depended on whatever grass had been produced in 1982 and on the woody plants of the area. The landscape of the Ferlo became, in large part, a sandy wasteland studded with low bushes. In 1983 the pastoralists evacuated their livestock to the south. In 1984 most of them remained in the south with their stock as it became clear to them that the rains had failed.

Apart from this marked annual variability in production, the maps also demonstrate something that ground samples could never do so clearly - the spatially erratic nature of production in the Sahel. In 1980 to 1982 the general north-south increase in production is apparent, but this trend is overlain by many local irregularities. Steep production gradients (and even "cliffs") can be found between adjacent localities, reflecting the highly variable productivity of neighbouring pastures.

8.9 Use of the maps

The maps serve to give the Government and development agencies an immediate and reasonably accurate idea of the level of production achieved by the pastures from year to year. This information reaches the officials in a form which is immediately comprehensible and with a delay of between 2 weeks and a month after the end of the rains.

They may be used to forewarn administrators of likely movements of livestock later in the year. Thus in 1980, for example, it is clear that herdsmen in Tatki and Mbidi could be expected to move their herds south before the end of the dry season. This intelligence could serve to prepare other boreholes for an influx of livestock and to prepare the authorities responsible for animal health for likely migrations.

A third major use for the maps is to prepare the relevant authorities for grass fires in specific areas in the dry season. Active measures, such as limited early burning on the upwind side of firebreaks, can then be undertaken immediately in high-risk areas, thus preventing the disastrous fires which afflict the area (GEMS 1986c).

Figure 17a and 17b: Biomass of the grass layer of the Ferlo at the end of the rainy seasons of 1980 and 1981 .

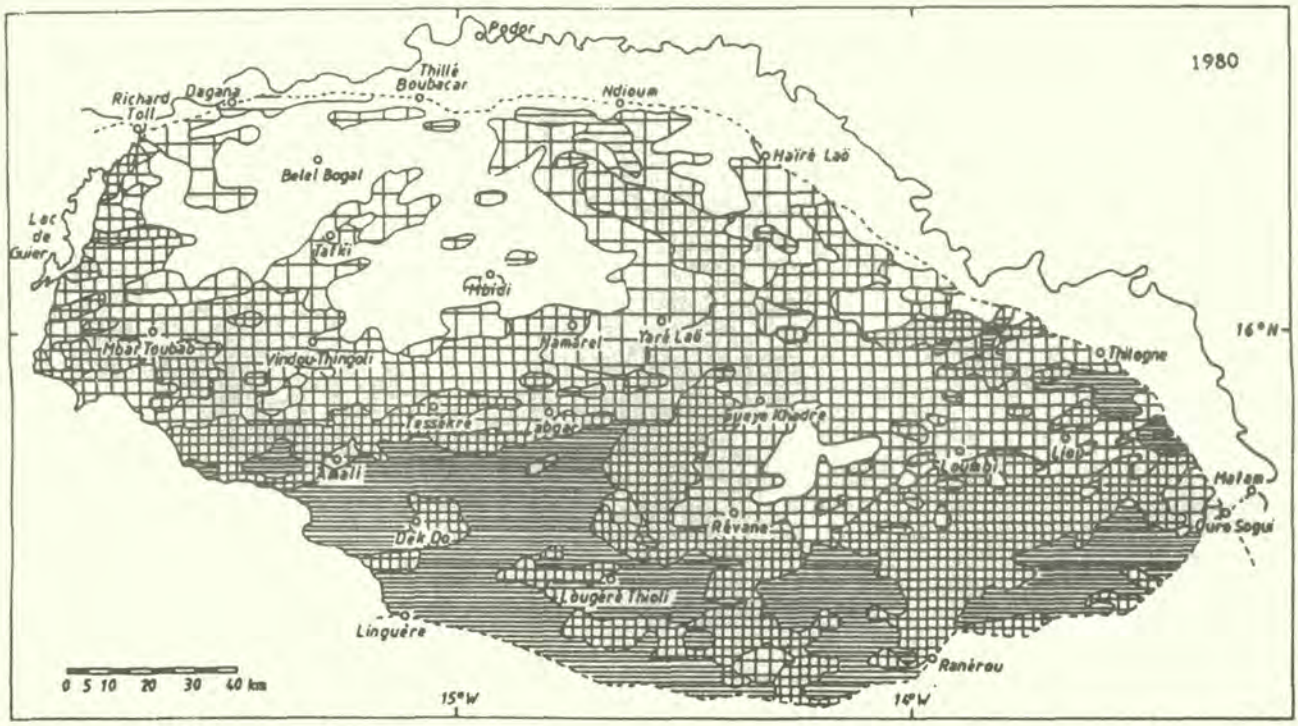

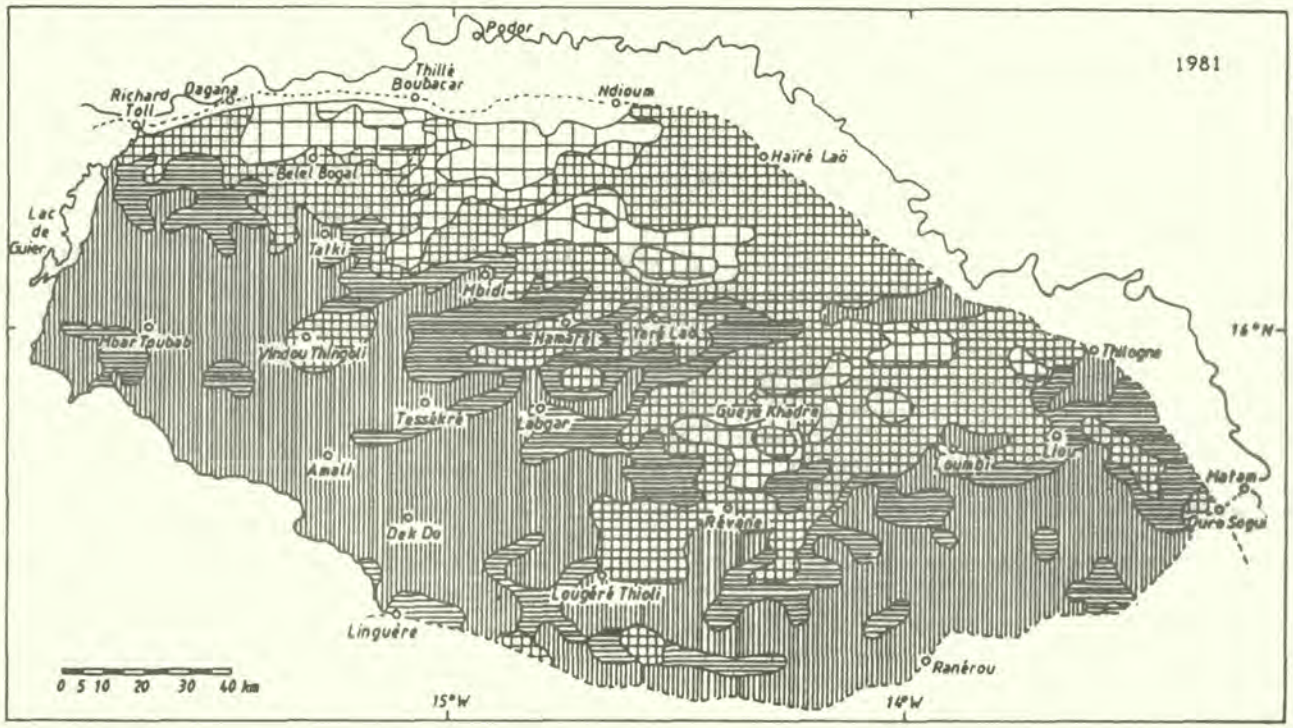

Figure 18a and 18b: Biomass of the grass layer of the Ferlo at the end of the rainy seasons of 1982 and 1983

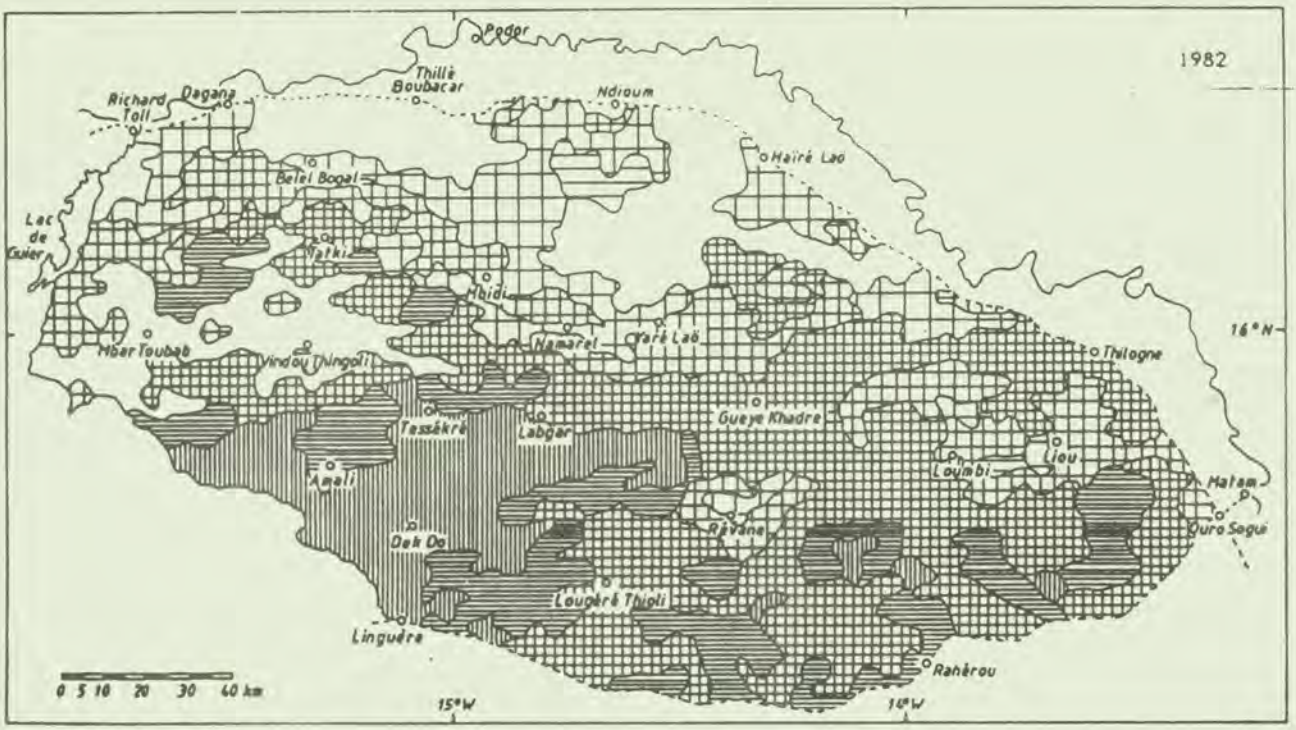

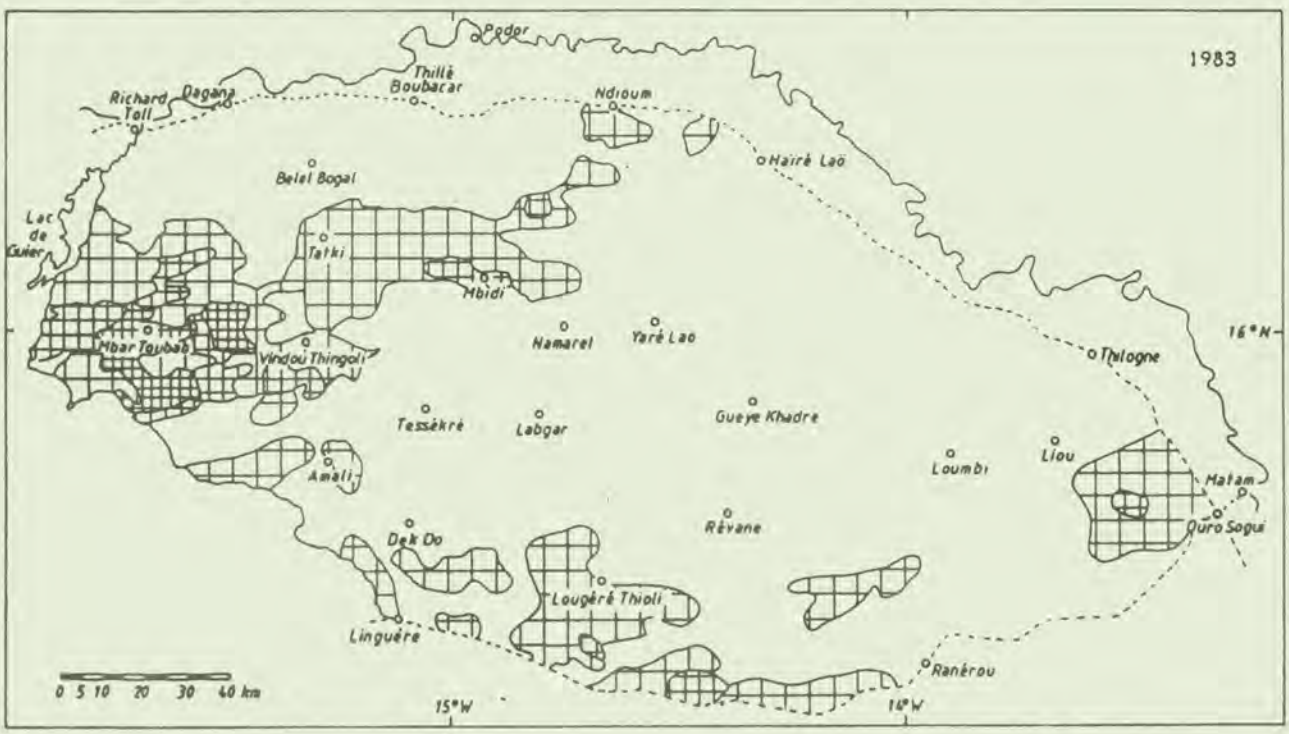

Figure 19a and 19b: Biomass of the grass layer of the Ferlo at the end of the rainy season 1984 and key to Figures 17-19

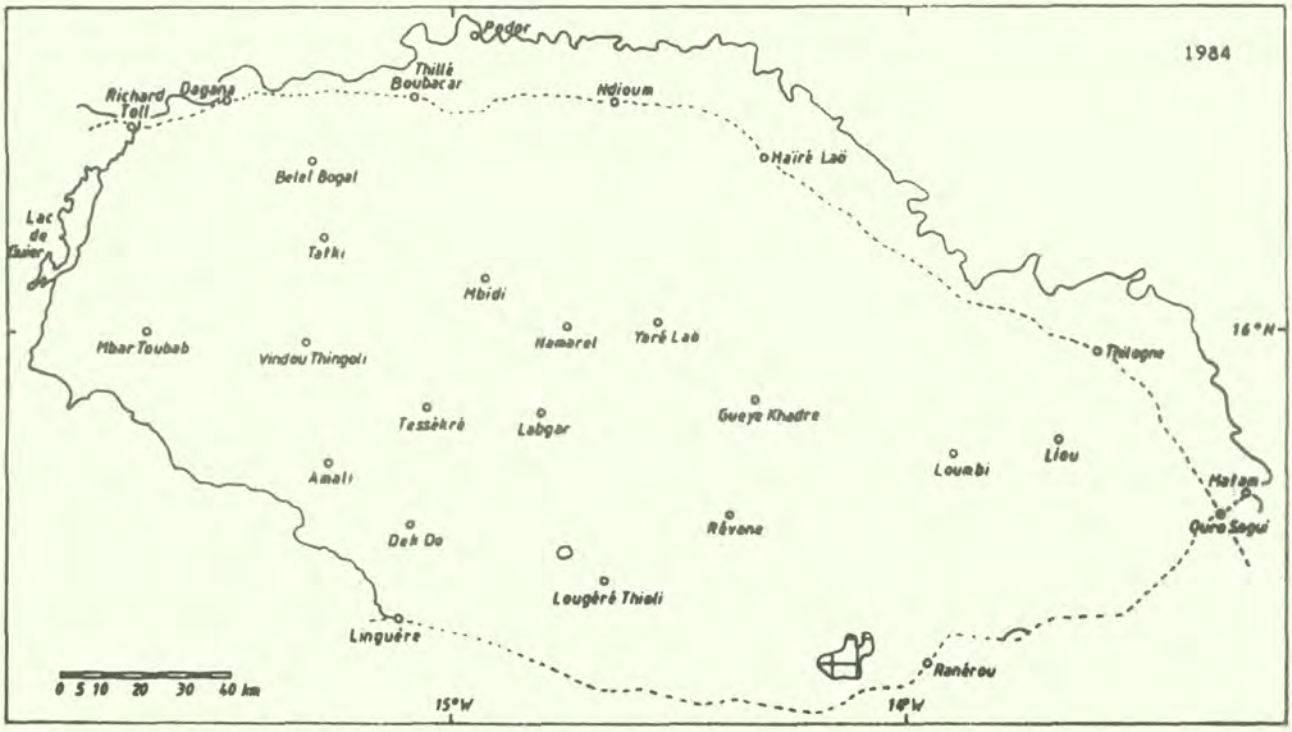

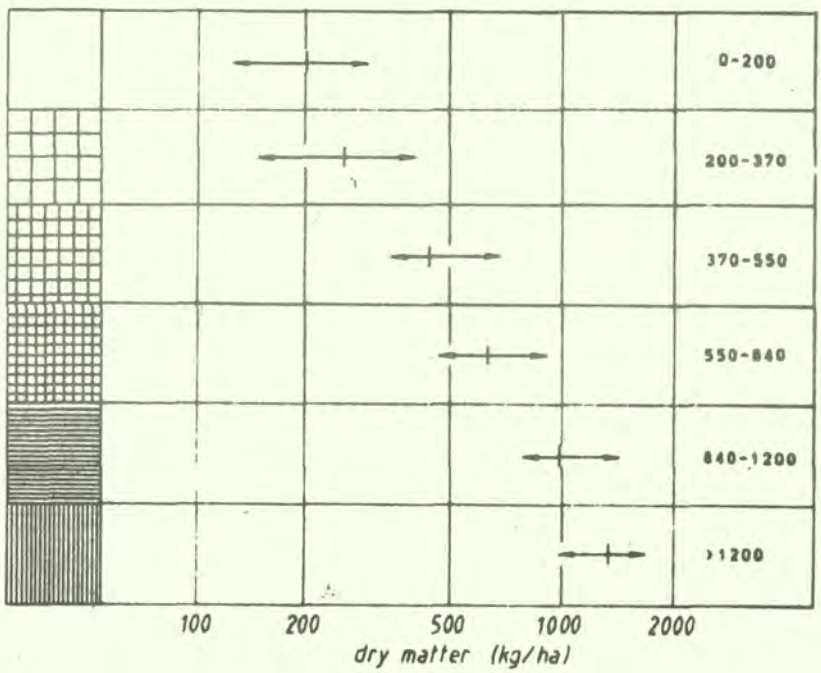

As a series of maps builds up over the years, it can be used by development agencies to understand and quantify the inherent variability of production in different parts of the zone. This information can then be used in feasibility studies before projects are launched.

9 Discussion

The quality of the sward, largely determined by species composition, is of course important in determining grazing capacity or stocking rates. Nevertheless, in the Sahel, biomass is often the primary factor, and any technique which makes it easier to collect data on biomass is highly desirable.

The NDVI may not give a good estimate of the dry weight of any single plot, but since clipping and weighing takes at least 10 times as long as making a single reading of the biomass, it is likely that by taking several radiometric readings of different samples in the area, a good mean estimate of the biomass can be had with less effort than is involved in clipping.

However, estimates of dry weight made with the NDVI are likely to be marginally worse than visual estimates depending either on height-times-cover or on cover-times-greenness. Since visual estimates take no more time and, since they use only the expertise of the observer, cost less than do radiometric ones, there is therefore a legitimate question to be posed and answered: is the hand-held radiometer a useful device in the pastures of the Sahel?

The principal advantage of the NDVI over any visual estimate is that the radiometer will presumably give the same results when used on the same plot under identical conditions by any two operators, but the same two observers may well disagree on the visual estimates of height and percent cover. The radiometric measurements are therefore intrinsically repeatable, while the visual estimates are not. A second advantage, more psychological than scientific, is that readers of the resulting reports are perhaps more likely to he persuaded by numbers emitted by an electronic instrument than they are by the "guesses" of observers, however educated. These arguements apply equally to the hand-held and airborne radiometers.

The lack of apparent effect of sun angle on naked earth does not necessarily imply that it is unimportant in radiometric measures of the vegetation, for which the sun angle will interact with the leaf angle and aspect. However, a study carried out by ILCA (Lamprey and de Leeuw 1986) suggests that sun angle may have little influence on the NDVI for mixed species swards in semi-arid pastures in Kenya, provided that the sun is high in the sky.

The results presented here show little inter-specific difference in the radiometric response of different grass species of sahelian pasturelands, and little improvement in the accuracy of radiometric estimates of biomass if samples are classed according to the dominant species. For most ecological monitoring in similar environments it is

therefore probably sufficient to record whether or not the dominant species is a grass. This implies that airborne measures taken over sahelian grasslands will probably give reasonably accurate estimates of the biomass of swards, irrespective of their species composition.

Both the hand-held and airborne radiometers are therefore potentially useful devices for the evaluation of the green and dry biomass of pasturelands. For many applications the hand-held radiometer may be more useful than clipping and weighing the biomass in plots, which, it should be said, poses its own problems of sampling and interpretation (GEMS 1986d). Improved estimates of biomass can probably be obtained by collecting radiometric data on the same plots, or in the case of airborne surveys, along the same transects, at several occasions during the growing season. The resulting readings can then be used to derive a single "integrated" score over the growing season which is more closely correlated with end-of-growing-season biomass than is any single reading.

If the hand-held radiometer will alleviate some of the work involved in collecting ecological ground data, satellite radiometry for monitoring standing grass-layer biomass clearly has considerable potential in the Sahel (Figure 22a), an area of limited accessibility and in which accurate ecological information is generally difficult to collect.

The pastoralists in any given area quickly discover, by word of mouth, where the good pastures are to be found, but the technique of satellite-based maps allows the Government and other agencies to learn, almost as quickly as the pastoralists themselves, a great deal about the productivity of remote parts of the country. Furthermore, while the pastoralists learn about the condition of distant pastures in general terms, the user of these maps has an instantaneous and quantitative view of the whole area.

The zone is characterised by steppe and savanna vegetation, in which the vertical projection of the canopies of woody plants cover around 10-30% of the surface. The satellite-borne instrument receives radiation reflected from all parts of the pastures, woody plants and grass layer plants alike. The image is therefore the result of a composite response, to which the quantitative contribution of the woody plant cover is as yet unknown. Undoubtedly, the accuracy of the information collected by the AVHRR and related to the grass layer is nevertheless more accurate in this region of thorn steppe and savanna with scattered woody plants (Figure 22b) than it is in the forested areas to the south. As far as Africa is concerned, therefore, satellite-based monitoring of grass-layer plants is perhaps at its most useful in the annual grasslands of the Sahel and in ecologically similar regions to the south of the continent.

In the Sahel the problem of woody plant cover is however compounded by the frequently observed tendency for grass to grow more vigourously under woody plant canopies than elsewhere; some of the most productive parts of the pastures are therefore invisible (or perhaps partly visible through woody plant canopies) to the radiometer in orbit. It may be argued that sahelian livestock make extensive use of woody plants in

Appendix 1: Glossary of terms connected to remote sensing and image processing.
An extensive list of terms used in remote sensing is given in Johannsen and Sanders (1982).

Absorptance: the fraction of incident electromagnetic energy which is transformed into chemical, heat or electrical energy.

Active: used to describe a remote sensing instrument which acquires information about a distant object by emitting electromagnetic radiation and measuring the intensity of the reflected energy in selected wavebands. Radar is an example of an active remote sensing device.

Aeroticule: particle or aerosol in the atmosphere.

Affine transformation: a mathematical technique by which all values in the original data are altered to give other values. The transform is one-to-one, in that any unique value in the original data corresponds to a unique value in the transformed data.

Albedo: the ratio of radiation reflected from a surface to the incident radiation summed across all wavebands. The source of the incident radiation is normally the sun.

Aphelion: point of orbit furthest from the sun.

Apogee: point of greatest separation of an orbiting satellite from the earth's surface.

Ascending mode: used to describe that part of the orbit of a polar-orbiting satellite over which the satellite is travelling northwards.

Azimuth: angle between the vertical plane through an object and an observer and a given direction (normally that formed by the plane through the observer and the terrestrial axis). The sun azimuth at the time a scene was recorded is the angle between the vertical plane through the sun and the centre of the scene and the plane through the centre of the scene and the terrestrial axis.

Backscatter: the scattering of radiation towards its source (where "towards" describes any direction forming an acute angle with the incident ray).

Band: a defined portion of the electromagnetic spectrum.

Band-pass: used to describe radiometer which measures one or more distinct bands selected from the electromagnetic spectrum.

Channel: band.

Colour-composite: adjective to describe an image made up from separate superimposed and registered images, each of which represents the intensity of energy received in a single waveband. Each of the component images is printed in a different colour to give an final product in several false (or, occasionally, simulated natural) colours.

their diets, and that the involuntary integration of the contribution o woody plants in the estimates of fodder biomass is therefore, by serendipity, appropriate. This is of course unsatisfactory and detaile research on the effect of the woody plant's contribution to the sahelia AVHRR data is shortly to start (Tucker pers comm).

Although radiometric indices derived from the hand-held radiometer exhibited wide variability for a given biomass, the relationship betwee the response of the satellite NDVI and the grass biomass sampled on the ground is apparently yet more erratic. This lack of close correspondence between the radiometric values and biomass presumably arises at least in part from the difficulty of gathering a representative sample of the mean biomass over an area the size of a pixel, that is, of the order of a square kilometer, from a few square metres of clipped grass. This topic is treated in some detail in GEMS (1986d), which includes a suggested sampling strategy for the calibration of AVHRR NDVI images.

The problem of registring successive images to create a single integrated image has been touched on in this document. In the Ferlo, registration of satellite images to ground features is relatively easy, since the coastline, the Lac de Guiers and the River Senegal may be use for reference. For most other areas of the Sahel the problem would be considerably more difficult.

The observation that NDVI classes are more highly correlated with latitude than sampled biomass in years of reasonable primary production tends to support the idea that the lack of fit derives largely from the non-representativity of the samples. If this is true it follows that i the Sahel at least, satellite-based estimates of primary production may be more accurate than are ground-based ones.

A further difference between the values of NDVI derived from the hand-held and satellite radiometers concerns their magnitude. Values of the NDVI from hand-held radiometers are roughly in the range 0.2 to 0.6, while those of the satellite-borne instrument are generally between 0 and 0.3. Although the Project did not have access to the raw data, it may be assumed that the main factor in this reduction was a relative diminution in the intensity in the Infrared received by the satellite.

If this is the case, which seems reasonable since the atmosphere absorb red and infrared light to different degrees, then much noise is being introduced into the satellite data, with the consequence that images will then have to be calibrated by field trips and ground data each year, as atmospheric conditions vary.

Contrast-stretching: term used in image processing and analysis to describe the process of altering the data by increasing the distance between successive values in the original data. Thus the values 175, 200, 225 might be altered to 50, 150, 250. The process is intended to enhance the contrast in the final image, making interpretation easier.

Density (of a part of an image): the opaqueness of that part of the image. See grey scale.

Density slicing: action of reducing the number of tones on an image by grouping similar tones into a single class. By extension, action of reducing range of numeric values to a few non-overlapping classes.

Descending mode: used to describe that part of the orbit of a polar-orbiting satellite over which the satellite is travelling southwards.

Detectability: an object is detectable on an image if an observer can state that it is present in the image. It may be possible to detect objects that cannot be identified, and to detect objects that are smaller than the resolving power of the sensor.

Dynamic range: the range of values of energy levels that a sensor can detect, measured by dividing the maximum measurable signal by the minimum: the number of gradations in the grey scale of an imaging device.

Edge enhancement: the automated process of detecting regions in an image in which near-neighbouring values change rapidly from one level to another, and assigning new values to pixels such that the rate of change between one level and the other becomes more pronounced. This has the effect of making the boundary between the two areas more sharply defined.

Electromagnetic spectrum: range of wavelengths of radiation including radio, microwaves, infrared, visible, ultraviolet, and gamma, in which electric and magnetic fields vary simultaneously.

Emittance: the radiation of electromagnetic energy from a source

Exitance: the quantity of electromagnetic energy leaving an object per unit area of its surface. Usually measured in watts per square meter.

False colour: used to describe images in which the colours are chosen to be dissimilar to the natural colours of the objects depicted. The standard Landsat false colour image shows band 4 in shades of blue, band 5 in green and band 7 in red.

Gaussian frequency distribution: random errors or fluctuations in the results of scientific experiments frequently follow a distribution which approximates the Gaussian (or Normal) form, a continuous, symmetric, bell-shaped distribution completely defined by its mean μ and its variance σ^2. The most important probability density function in statistics, it takes the form

$$y = \frac{e^{(-(x-\mu)^2/2\sigma)}}{\sigma\sqrt{(2\pi)}}$$

Geometric accuracy: degree to which scale remains constant over the image.

Geostationary: adjective to describe a satellite whose orbital period about the earth coincides with the period of the earth about its axis, and whose apparent position relative to a point on the earth's surface does not change. Meteosat is a geostationary satellite.

Grey scale, tonal scale, or saturation scale: The division of a spectrum of grey tones ranging from white to black into exclusive and contiguous slices or ranges of density. The number of classes into which grey scales are sliced is normally some power of 2, such as 64 (band 7 of TM), 128 (bands 4,5 and 6 of TM), or 256 (MSS).

Ground data: data collected in the field which is used to interpret or calibrate data collected from airborne or satellite-based sensors.

Ground resolution distance: a measure of the detail available on an image. This depends on the scale of the image (1:S) and the resolution R of the image in lines per millimetre, and is calculated by:

$$GRD = S/(R \times 1000)$$

Ground resolution element: the smallest spot on the ground theoretically resolvable by a sensor. This depends on the altitude A of the platform, the wavelength W of the electromagnetic energy being sensed, and the diameter D of the sensor, and is calculated by:

$$GRE = 1.2*AW/D$$

Ground trace: see swath width

Ground truth: a misleading term which should be replaced by "ground data", "ground control" or "ground observations".

Histogram equalization: technique in image processing in which equal numbers of pixels are assigned to each density slice.

Identifiability: the capacity to detect, recognise and categorise a region in an image.

Image: The visual reconstruction of a scene scanned and recorded by a remote sensing system. An image is a raster, whose elements are pixels, built up from individual scan lines. An image is not a photograph (although a photograph may show an image!).

Image enhancement: the process of improving the visual quality of an image or of bringing out certain features or characteristics of the image.

Image processing: techniques of computer-assisted image enhancement and classification intended to increase the accuracy and informativeness of the depiction of a scene.

Image uniformity: degree to which surfaces of equal radiance, in different parts of a scene, are represented by the same signal level in the processed data.

Instantaneous field of view: the solid angle viewed by a sensor at any one moment, or the equivalent area on the ground.

Irradiance: the quantity of incident electromagnetic energy per unit area of the surface. Usually measured in watts per square meter.

Lambertian surface: a surface which reflects radiation equally in all directions.

Land form: morphological description of surface; principally slope angle and aspect, and may include elevation and the form of the profile or surface.

Landform: geomorphological description of area.

Leaf area index: leaf area per unit ground area.

Linear array: a device constructed of several sensors arranged at equal distances along a straight line.

Mie scatter: scattering due to particles whose diameters are roughly equal to the wavelength in question.

Multilevel sampling: technique of combining remotely sensed data from various platforms with data from other platforms, including ground data.

Multispectral: used to describe a remote sensing instrument which detects and measures energy from more than one band of the electromagnetic spectrum.

Multitemporal: used to describe repeated studies of the same area.

Nadir: the point on the earth's surface vertically below the observer or satellite.

Noise: random or systematic deviations in data which reduce its precision and usefulness.

Non-imaging: used to describe a radiometer which is not designed to construct an image of a sensed scene.

Non-selective scatter: scattering due to particles whose diameters are several times the wavelengths in question.

Normal frequency distribution: since the adjective "normal" implies "usual" or "typical", the preferred term is "Gaussian" (qv), except

where the use of "Gaussian" makes the text clumsy and "Normal" is unambiguous.

Normalization: term in image processing used to describe the division o values of one band by the sum of values from two other bands.

Normalized difference: the difference between values from two bands divided by their sum.

Oblateness: the degree to which an elliptical orbit deviates from a circle.

Ortho- : used to describe an image or photograph which has been corrected for the slope of the terrain, and for the tilt of the axis of the apparatus used to detect and record the image or photograph, in suc a way as to have a uniform scale across the scene.

Panchromatic: used to describe a sensor sensitive to most or all of the spectrum of visible light

Passive: used to describe a remote sensing instrument which detects and measures electromagnetic radiation which was originally emitted by a source other than the instrument itself.

Perigee: point of closest approach.

Perihelion: point of orbit closest to the sun.

Period: the time taken for a satellite to complete one orbit.

Photon: quantum of electromagnetic radiation, whose energy is proportional to the frequency of the radiation.

Pixel: a contraction of "picture element"; the smallest fragment of an image, having a single value for each recorded waveband.

Platform: the vehicle carrying the sensor. Typical platforms for remo sensing are: satellite, aircraft, mobile gantry, tripod and the human hand.

Polar orbit: course of a satellite oriented so that it passes over the north and south poles of the earth. Many earth resources satellites have near-polar orbits, because such a track allows the satellite to pass over different parts of the planet as the earth rotates slightly its axis in the interval between each successive orbit.

Principal components analysis: multivariate statistical technique used in image processing to derive a final image by weighting and combining the linear contribution of several original bands.

Push-broom: used to describe a sensor made up of a linear battery of aligned and radiometrically identical radiometers each of which receiv radiation from adjoining but not overlapping areas across the range. The instrument records as the vehicle moves along the track, in a mann likened to that of a broom pushed along the ground.

Radiance: the intensity of radiant flux in a given direction. Radiation from a surface is emitted in all directions. Radiance is therefore measured as the intensity of radiant flux through a cone based on the surface of the source, and is given the units of watts per steradian per unit area of the emitting surface.

Radiant flux: the amount of radiant energy reaching a surface or sensor in a given time. Usually measured in joules per second or watts.

Radiometric resolution: the precision with which radiance is represented in the data. This depends on the characteristics of the sensor and on the subsequent treatment of the data.

Raleigh scatter: scattering due to particles (such as gas molecules) whose diameters are much smaller than the wavelength in question. Short wavelengths are scattered more than longer ones, in proportion to the fourth power of their frequency.

Range: direction in the plane of the earth's surface at right angles to the track of the vehicle.

Raster: the pattern of scanning lines on the screen of a cathode ray tube. By extension, a matrix of cells each of which has a value normally independent of its coordinates in the raster but corresponding to some measured parameter.

Ratioing: the derivation of a new value for a pixel from the ratios of values in two wavebands for that pixel.

Real time: used to describe a system used to inspect and process data as the data are being collected. Also, by extension, used to describe data made available to the user a short time after they were collected.

Recognisability: the property possessed by an object in an image if it can be broadly classified but not necessarily identified.

Reflectance: the proportion of electromagnetic energy incident on a surface which is reflected by that surface.

Registration: the process of accurately aligning all elements of an image or photograph on a mapped projection of the earth's surface or on another image or photograph.

Remote sensing: the detection and recording of electromagnetic information by means of a manmade sensor which is not in contact with the object from which the information is collected.

Réseau: the intersection of grid-lines printed on images or aerial photographs. These cross-hairs allow the user to register the image or photograph accurately.

Resolution: see Radiometric resolution, Spectral resolution, Spatial resolution and Temporal resolution.

Resolving power: the minimum distance apart at which two objects are visually separable on an image.

Saturation scale: see grey scale

Scanner: an instrument used to collect reflected energy from successive parts of the scene (from one side of the swath to the other) and to direct that energy to one or more detectors. Most scanners make use of a telescope and a rotating prism or mirror.

Scattering: the alteration in direction (and usually intensity) of radiation by particles in the atmosphere. See mie, raleigh and non-selective scatter.

Scene: data collected in a standard section of the swath of a sensor. The data are influenced by the spectrum of the energy source, the spectral effects of the atmosphere, and the spectral characteristics of the surface. A Landsat MSS scene contains 2340 scan lines, 3240 pixels per line, and the raw data contain four values for each pixel. The scene covers 185 x 185 sq km.

Sidelap: the area that is common to two adjoining swaths. In a polar orbiting satellite the sidelap is greater near the poles than it is near the equator.

Signal-to-noise ratio: the level or intensity of the useful information contained in data divided by the level or intensity of random fluctuations (noise) in the data.

Skew: distortion from a symmetric shape. Two different types of skew are recognised in image processing. Firstly, asymmetric images are skew: thus, for example, Landsat scenes are skew in that they are parallelograms, not rectangles, as a result of the earth's rotation under the satellite and the movement of the satellite along the track during the time taken to scan the scene. Secondly, in the statistical treatment of data, skew measures the asymmetry of frequency distributions.

Spatial resolution: the minimum distance between two objects at which the objects appear separate on the image. Spatial resolution is not the dimension of the smallest object that can be seen on the image. It is affected by the shape of the objects, the spectral contrast between objects and their background, and the signal-to-noise ratio.

Spectral response: the relative intensities of various wavelengths of reflected electromagnetic energy, whose characteristics under given illumination depend to some extent on the characteristics of the surface from which the radiation is reflected.

Spectral resolution: the width and part of the electromagnetic spectrum which is detected by an instrument.

Spectral signature: the supposedly constant spectral response of a giver surface. Since, in fact, many factors influence the spectral response of an object, the supposedly constant signature changes with external conditions. The term is normally better replaced by the preferable "spectral response".

Specular reflection: reflection of radiation without scattering or diffusion, as from a perfect mirror. In the case of active sensors, specular reflection of the emitted signal is usually in a direction such that the reflection cannot be detected by the sensor.

Sun angle: angle of the sun above the horizon as measured from the centre of the scene or by an observer on the ground.

Sun-synchronous: used to describe an orbit in which the satellite passes vertically above a given latitude at the same solar (as opposed to sidereal time each day. This has the advantage that the sun illumination remains the same for repeated images of the same scene taken at annual intervals.

Supervised: image processing term used to describe a computer-assisted classification of an image involving the selection of training areas by the operator.

Swath: the strip of the earth's surface which is surveyed by the scanner.

Swath width: the width of the strip on the earth's surface which is surveyed by the scanner in an aircraft or satellite.

Synthetic aperture radar: a side-looking terrain-imaging radar in which the processing of the reflected signal takes account of the duration over which the emmitted pulses are returned in such a way that resolution is made independent of wavelength, range and the dimensions of the antenna.

Target: the surface providing the source of reflected or emitted radiation measured by the remote sensing system: usually a portion of the earth's surface.

Temporal resolution: the frequency with which an instrument collects data over a given area.

Tonal scale: see grey scale

Track: vertical projection of the trajectory of a vehicle on the earth's surface.

Training area: image processing term used to describe a section of an image selected by an analyst in computer-assisted supervised classification of a scene. The training area is usually chosen for its homogeneity and because the analyst knows what this section of the image represents on the ground. The software examines the spectral response of the pixels in the training area and uses its characteristics to identify other pixels with similar spectral responses.

Uncontrolled: used to describe an image which has undergone no correction for distortion.

Unsupervised: image processing term used to describe the computer-assisted classification of an image in which the software assigns pixels to clusters of similar pixels according to their spectral responses. There are several techniques by which the classification may be carried out.

Vidicon: a derivative of the television tube capable of storing visual information temporarily on a photosensitive surface. In the return-beam vidicon (RBV) this stored image is then scanned by an electron beam and the resulting signal digitized.

Window: Region of the electromagnetic spectrum in which the atmosphere is relatively transparent.

Appendix 2: Acronyms and abbreviations commonly found in remote sensing literature. A more complete list of acronyms used in remote sensing is given in Johannsen and Sanders (1982). This list also contains a few other acronyms used in this report.

AMSU	Advanced Microwave Sounding Unit
ATM	Airborne Thematic Mapper
ATN	Advanced TIROS-N
AVCS	Advanced Vidicon Camera System
AVHRR	Advanced Very High Resolution Radiometer
CCD	Charge-Coupled Device
CCT	Computer-Compatible Tape
CNES	Centre National d'Etudes Spatiales
CRT	Cathode Ray Tube
CSIRO	Commonwealth Scientific and Industrial Research Organization
DAS	Differential Absorption and Scattering
DCS	Data Collection System (Landsat)
EARSEL	European Association of Remote SEnsing Laboratories
ECHO	Extraction and Classification of Homogeneous Objects (algorithm)
ELAS	Earth resources Laboratory Applications Software
EMS	ElectroMagnetic Spectrum
ERDAS	Earth Resources Data Analysis System
EREP	Earth Resources Experiment Package
EROS	Earth Resources Observation System
ERTS	Earth Resources Technology Satellite (now Landsat)
ESA	European Space Agency
ESSA	Environmental Science Services Administration
ETC	Earth Terrain Camera
FOV	Field Of View
GAC	Global Area Coverage
GDTA	Groupement pour le Développement de la Télédétection Aérospatiale
GISS	Goddard Institute for Space Studies
GMT	Greenwich Mean Time
GOES	Geostationary Operational Environmental Satellite
GRD	Ground Resolution Distance
GRE	Ground Resolution Element
GSFC	Goddard Space Flight Center
HIRS	High resolution InfraRed Sounder
HRV	High Resolution Visible
IFOV	Instantaneous Field Of View
ILCA	International Livestock Centre for Africa
I/O	Input/Output
IR	InfraRed
IRLS	InfraRed Line Scanner
JPL	Jet Propulsion Laboratory
LAC	Local Area Coverage
LAI	Leaf Area Index
LARS	Laboratory for Application of Remote Sensing
LASER	Light Amplification by Stimulated Emission of Radiation
LIDAR	LIght Detection And Ranging
MASER	Microwave Amplification by Stimulated Emission of Radiation
MLA	Multi-Linear Array
MSS	Multi-Spectral Scanner
NASA	National Aeronautical and Space Administration

NDVI	Normalised Difference Vegetation Index
NOAA	National Oceanic and Atmospheric Administration
PAMIRASAT	PAssive MIcrowave RAdiometer SATellite
RADAR	RAdio Detection And Ranging
RBV	Return Beam Vidicon
R	Red
RR	(in this report) Reflected Radiation
SAR	Synthetic Aperture Radar
SARSAT	Synthetic Aperture Radar SATellite
SLAR	Side Looking Airborne Radar
S/N	Signal-to-Noise ratio
SONAR	SOund NAvigation and Ranging
SPOT	Système Probatoire d'Obsérvation de la Terre
SST	Sea Surface Temperature
TIR	Thermal InfraRed
TIROS	Television and InfraRed Observation Satellite
TM	Thematic Mapper
UV	UltraViolet
VDU	Visual Display Unit
VTR	Video Tape Recording
WB	WaveBand
WBVTR	Wide Band Video Tape Recorder

Bibliography

Daughtry C.S.T., K.P. Galio and M.E. Bauer (1983) Spectral estimates of solar radiation intercepted by corn canopies. Agronomy Journal 75:527-531

GEMS (1986a) Introduction to the Sahelian Pastoral Ecosystems Project. Global Environment Monitoring System Sahel Series No 1. UNEP/FAO

GEMS (1986b) Rainfall in the Ferlo (Sahelian region of north Senegal) since 1919. Global Environment Monitoring System Sahel Series No 2. UNEP/FAO

GEMS (1986c) Use of Light Aircraft in the Inventory and Monitoring of Sahelien Pastoral Ecosystems. Global Environment Monitoring System Sahel Series No 3. UNEP/FAO

GEMS (1986d) Sampling the Sahel. Global Environment Monitoring System Sahel Series No 4. UNEP/FAO

GEMS (1986e) Reduction in woody vegetation cover in the Sahel. Global Environment Monitoring System Sahel Series No 6. UNEP/FAO

Graetz D. (1985) The Perpendicular Vegetation Index. Paper presented to Workshop on Remote Sensing of Rangelands. GEMS/UNEP. Nairobi.

Holmes R.A. (1970) Field spectroscopy. Pp 298-323 In: Committee on Remote Sensing for Agricultural Purposes. Remote sensing with special reference to agriculture and forestry. National Academy of Sciences. Washington DC.

Johannsen C.J. and J.L. Sanders (1982) (Eds) Remote sensing for resource management. Soil Conservation Society of America. Ankeny, Iowa.

Kumar M. and J.L. Monteith (1982) Remote sensing of plant growth. In: Smith H. (Ed) Plants and the daylight spectrum. Pitman. London.

Lamprey R.H. and P.N. de Leeuw (1986) The use of NOAA-AVHRR imagery for rangeland monitoring.

Lee K. (1975) Ground investigations in support of remote sensing. Pp 805-856 In: Reeves R.G. (Ed) Manual of Remote Sensing. American Society of Photogrammetry. Virginia.

Le Houérou H. (1986) Pilot project on the Inventory and Monitoring of Sahelian Pastoral Ecosystems: Summary technical report. GEMS/UNEP/FAO

Pollard J.H. (1977) A Handbook of Numerical and Statistical Techniques. With examples mainly from the life sciences. Cambridge University Press. Cambridge.

Rouse J.W., R.H. Haas, J.A. Schell, and D.W. Deering (1973) Monitoring vegetation systems in the Great Plains with ERTS imagery. Pp 309-317 In: NASA Special Publication No. 351: Proceedings of the 3rd ERTS symposium.

Sharman M.J. and C.L. Vanpraet (1983) Mesure au sol de la production primaire par utilisation du spectroradiomètre. Pp 321-332 In: Vanpraet C.L. (Ed) Methodes d'Inventaire et de Surveillance continue des Ecosystèmes pastoraux sahéliens: Application au Developpement. Ministère de la Recherche Scientifique et Technique. Dakar.

Sokal R.R. and F.J. Rohlf (1969) Biometry. The principles and practice of statistics in biological research. WH Freeman and Co. San Fransisco.

Tucker C.J. (1979) Red and photographic infrared linear combination for monitoring vegetation. Remote Sensing of Environment 8:127-150

Tucker C.J. (1980) A critical review of remote sensing and other methods for non-destructive estimation of standing crop biomass. Grass Forage Science 35:177-182

Tucker C.J., C.L. Vanpraet, E. Boerwinkel and A. Gaston (1983) Satellite remote sensing of total dry-matter production in the Senegalese Sahel. Remote Sensing of Environment 13:416-474

Vanpraet C.L., M.J. Sharman and C.J. Tucker (1983) Utilisation des images NOAA pour l'estimation de la production primaire en milieu sahelien. Pp 299-319 In: Vanpraet C.L. (ed) Methodes d'Inventaire et de Surveillance continue des Ecosystèmes pastoraux sahéliens: Application au Developpement. Ministère de la Recherche Scientifique et Technique. Dakar.